Ore Geology Reviews 125 (2020) 103683

Contents lists available at ScienceDirect

Ore Geology Reviews

journal homepage: www.elsevier.com/locate/oregeorev

# Contribution of crustal and mantle sources to genesis of Sn, B and Pb-Zn deposits in South Sikhote-Alin subprovince (Russian Far East): Evidence from high–precision MC-ICP-MS lead isotope study

A.V. Chugaev[a,b,*], I.V. Chernyshev[a], V.V. Ratkin[c], V.G. Gonevchuk[c], O.A. Eliseeva[c]

[a] Institute of Geology of Ore Deposits, Petrography, Mineralogy and Geochemistry, Russian Academy of Sciences, Staromonetny Lane, 35, Moscow 119017, Russia
[b] Institute of Geology and Petroleum Technologies, Kazan Federal University, 4/5 Kremlyovskaya, Kazan 420008, Russia
[c] Far Eastern Geological Institute, Far East Branch, Russian Academy of Sciences, 159, Avenue of the 100th Anniversary of Vladivostok, Vladivostok 690022, Russia

ARTICLE INFO

*Keywords:*
Lead isotopes
Sn
B and Pb-Zn deposits
South Sikhote-Alin metallogenic subprovince

ABSTRACT

South Sikhote-Alin metallogenic subprovince (SSAP) is located in the southern part of the Sikhote-Alin orogenic belt. It encompasses more than one hundred well-known deposits and occurrences of boron, tin, lead, and zinc. These deposits have been genetically related to the Late Cretaceous and Paleocene granitoid magmatism. Pb isotope composition was measured using the MC-ICP-MS method in 20 SSAP deposits. Pb isotope ratios (48 samples of galena) vary within narrow limits: $^{206}Pb/^{204}Pb$ ranges from 18.321 to 18.474, $^{207}Pb/^{204}Pb$ – 15.608–15.655, and $^{208}Pb/^{204}Pb$ 38.601–38.796. The high degree of homogeneity of the Pb isotope composition and absence of correlations between the lead isotope characteristics of the deposits, on the one hand, and the age and type of ore mineralization, on the other, indicate the presence of a regional uniform Pb source for all the SSAP deposits. The results of Pb-Pb studies of the different rocks of the SSAP suggest that the source was most likely the Mesozoic sedimentary sequences of the Sikhote-Alin accretionary complexes. In turn, individual lead isotope characteristics of the SSAP deposits are caused by varibale contribution of mantle source to the overall balance of lead.

## 1. Introduction

Sources of matter and their relative contribution to formation of ore mineralization of various type and genesis is one of the key issues for understanding the evolution of ore-forming processes and their relationship with the main stages of geological development of metallogenic provinces. One of the most effective and universal approaches to solve this issue is to study common lead isotope variations in rock and ore samples using inductively coupled plasma multicollector mass-spectrometry (MC-ICP-MS; Rehkämper and Halliday, 1998; Collerson et al., 2002; Chernyshev et al., 2007; Kamenov et al., 2002; Chugaev et al., 2013a; Standish et al., 2014; Chernyshev and Shpikerman, 2001; Chernyshev et al., 2018). In recent years, this approach (Rehkämper and Halliday, 1998) as a leading analytical method for the lead isotope geochemistry has essentially superseded the thermal ionization mass spectrometry technique (TIMS), which was traditionally used for more than 40 years. The high-precision version of the MC-ICP-MS method includes lead isotope analysis from solutions and mass-bias correction of measured Pb isotope ratios using a standard added to the samples – thallium isotopes $^{205}Tl$ and $^{203}Tl$. The MC-ICP-MS approach surpasses the traditional TIMS by an order of magnitude better precision with error ( ± 0.02–0.03% vs. ± 0.2–0.3% for TIMS). This allows quantitative recognition and interpretation of small (0.05–0.5%) variations in Pb isotopic composition, as well as reliable determination of regional differences and their correct use for geological and geochemical purposes.

The high-precision Pb isotope data for this study have been collected on samples from the South Sikhote-Alin subprovince (Russian Far East). It is located in the southern part of the Sikhote-Alin orogenic belt. The province encompasses more than one hundred well-known deposits and occurrences of boron, tin, lead, and zinc. These deposits have been formed in association with Late Cretaceous and Paleocene magmatism (Grebennikov et al., 2016). Despite long history of the study, the problem of the source/sources of the ore matter still remains one of the most controversial. At the same time, contribution of both crustal and mantle sources is assumed (Gonevchuk et al., 2011, Ratkin et al.,

* Corresponding author at: Institute of Geology of Ore Deposits, Petrography, Mineralogy and Geochemistry, Russian Academy of Sciences, Staromonetny Lane, 35, Moscow 119017, Russia.
*E-mail address:* vassachav@mail.ru (A.V. Chugaev).

https://doi.org/10.1016/j.oregeorev.2020.103683
Received 29 November 2019; Received in revised form 22 June 2020; Accepted 14 July 2020
Available online 18 July 2020
0169-1368/ 

2016a).

The first Pb-Pb data for ore deposits in the South Sikhote-Alin subprovince were obtained by TIMS technique ca. 35 years ago (Tomson et al., 1984). Those results showed a similarity of Pb isotope composition in deposits with different type of mineralization, driving the authors to conclude on geochemical uniformity of the source. This source has been defined as a common homogenous reservoir, commensurate with the territory of the southern Sikhote-Alin. According to the plumbotectonics model (Zartman and Doe, 1981), the source has lead isotopic characteristics of the orogenic reservoir. However, by that time the available isotopic and geological data did not allow to specify this conclusion and identify a certain source(s) of Pb in the ores. There are also single articles (Rasskazov et al., 2002; Rostovsky, 2005) that present limited Pb-Pb data for selected Sikhote-Alin deposits. The inconsistency of the published results and their wide variation indicate a significant contribution of analytical errors/inaccuracy that were not monitored and taken into account during the TIMS studies. For this reason, the data of Rasskazov et al. (2002) and Rostovsky (2005) are not discussed in this article.

This article contains results of Pb isotope composition study in 48 galena samples from 20 deposits of the South Sikhote-Alin. In particular, 13 extant duplicates of galena samples from the Tomson et al. (1984) collection have been re-analyzed. Lead isotopes have also been determined in 7 feldspar samples from granitoids of various ages and in the Early Cretaceous sedimentary rocks (10 whole rock samples) from the South Sikhote-Alin.

## 2. The Sikhote-Alin orogenic belt (SAOB): Geological overview

### 2.1. Tectonic pattern and geological history

The South Sikhote-Alin metallogenic subprovince (SSAP) occurs in the southern part of the Sikhote-Alin orogenic belt (SAOB) in the Russian Far East.

The orogenic belt is a collage of terranes, comprising fragments of the Jurassic to Early Cretaceous accretionary prisms, Early Cretaceous island arcs, as well as sedimentary units of strike-slip-related turbidite basins (Fig. 1). The collage was formed during few stages (Fig. 2). The Samarka accretionary wedge terrane has been formed in the Early Jurassic at the eastern margin of the Bureya-Jiamusi-Khanka superterrane (BJKT) as a result of subduction of the Paleo-Pacific plate (Liu et al., 2017). More than 11 km thick sedimentary unit has been accumulated in the Early Cretaceous (Berriasian to Albian inclusive) in the Zhuravlevka turbidite basin (Zhuravlevka terrane), extending southwards to the latitude of the North China Craton (NCC) (Golozoubov, 2006; Liu et al., 2017) under a transform-type boundary regime between the lithospheric plates. The NCC was the main source of debris into this turbidite basin. In the south of the Zhuravlevka basin (southwards of 32°N) near the NCC, the Early Cretaceous (Berriasian-Valanginian) accretionary wedge of the Taukha terrane was formed. During this time, the subduction was directed northward under the continent (Golozoubov, 2006). The Taukha rocks were sourced from the eastern NCC, including the Korean Peninsula (Liu et al., 2017). To the east of the Taukha basin at the latitude of c. 35°, N the Early Cretaceous Kema island arc terrane was formed (Didenko et al., 2018). At the end of the Early Cretaceous, the rock complexes of the Taukha and Zhuravlevsky sedimentary basins were deformed during left-lateral strike-slip displacement, driven by a transform-like translation of the oceanic plate relative to the continental margin. In Late Albian, terranes have been translated to their modern position in the SAOB. At the same time, the Kema island arc collided with the mainland, resulting in formation of the Sikhote-Alin orogenic belt (Khanchuk et al., 2016).

The SSAP are located within the Zhuravlevka and Taukha terranes. The Zhuravlevka terrane consists of the Berriasian-Albian clastic sequences (ca. 11 km) with tolleiitic basalts overlapped by late Tithonian oceanic cherts and mudstones at the base (Kemkin, 2006).

The Taukha terrane is an accretionary prism comprising Triassic-Jurassic cherts and basalts, as well as Early Cretaceous turbidites and olistostromes with blocks of Triassic limestones (Kemkin, 2006; Khanchuk et al., 2016). The total thickness of the sedimentary sequence reaches ca. 13 km. The accretionary prism rocks demonstrate a tectonio-stratigraphic regularity expressed in a triple repetition of the sequence. The accretionary prism comprises mostly Berriasian to Valanginian arkose sandstones and siltstone. Allochthons of tectonically imbricated oceanic rocks are, as a rule, sparse, yet reaching first tens of volume percent in some parts of the Taukha terrane (Golozoubov, 2006; Khanchuk et al., 2016).

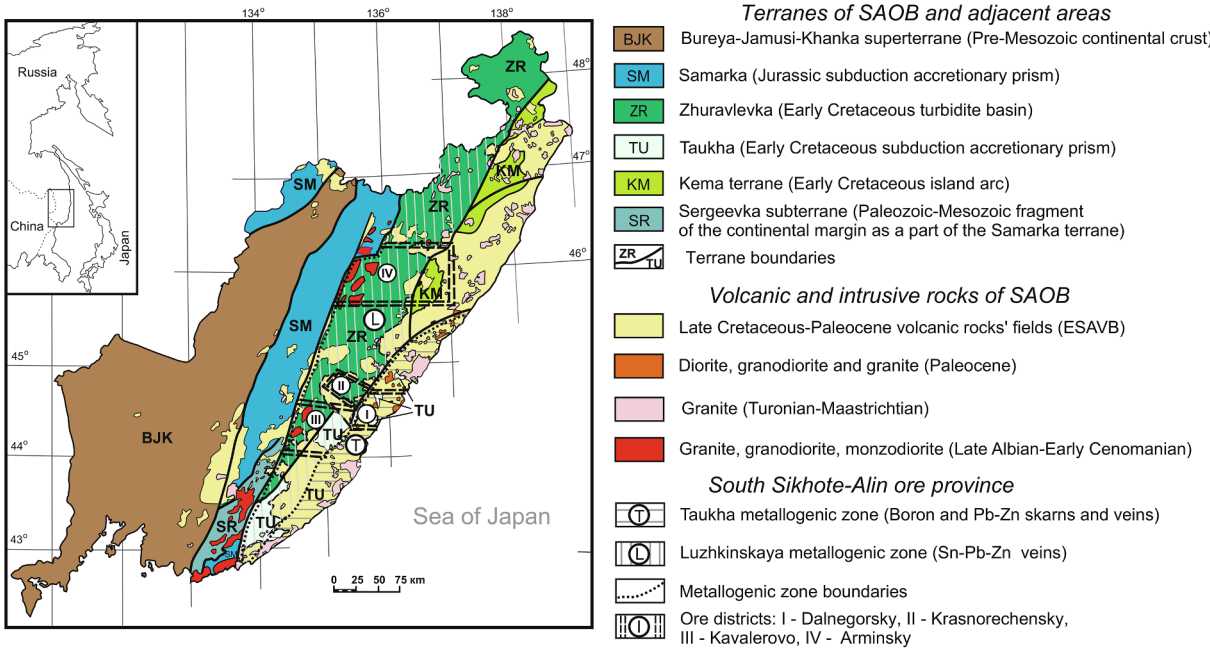


**Fig. 1.** Geological sketch of the Sikhote-Alin orogenic belt and position of the South Sikhote-Alin subprovince (Taukha and Zhuravlevka metallogenic zones) and studied districts on the terranes' diagram within Primorsky Krai of the Russian Federation, (modified after Grebennikov et al., 2016).

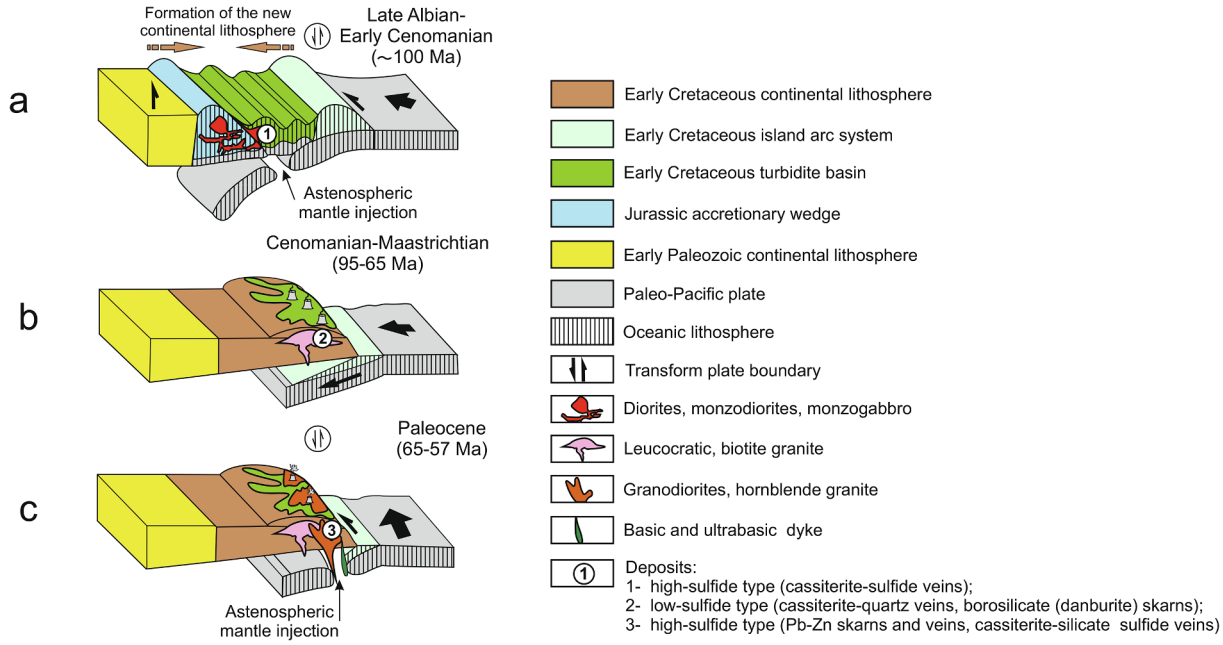


**Fig. 2.** Model showing a paleogeodynamic Late Albian – Paleocine reconstruction of the Sikhote-Alin area (modified after Grebennikov et al., 2016).

### 2.2. Magmatism and metallogenesis

Spatially and temporally, the SSAP deposits are closely associated with the Cretaceous-Paleocene magmatic complexes. The magmatic complexes include volcanic rocks and granitoids (Jahn et al., 2015; Khanchuk et al., 2016). Their formation can be subdivided into three stages by age and stages of tectonic evolution of the region in the Cretaceous and Paleocene (Grebennikov et al., 2016).

The first stage (late Albian to early Cenomanian) corresponds to the peak of magmatic activity at ca. 100 Ma in relation to the orogeny caused by collision of the Early Cretaceous Kema island arc with the continental margin (Khanchuk et al., 2016; Kruk et al., 2019). Synorogenic intraplate magmatism was caused by emplacement of an asthenospheric mantle into upper crustal levels, with intrusion of diorites, monzodiorites, and monzogabbro (Grebennikov et al., 2016; Kruk et al., 2019; Fig. 2a). The parental mantle melts were substantially contaminated with an upper crust material. At this time, numerous cassiterite-sulfide vein deposits were formed in association with intrusions of synorogenic monzonites. The peak ore formation, based on dating the hydrothermal alteration (Gonevchuk, 2002), took place at 95–90 Ma.

The second magmatic stage (Fig. 2b) occurred in Turonian-Campanian times (95–65 Ma) during restart of subduction of the Paleo-Pacific plate (Grebennikov et al., 2016). During this period, a giant (up to 3.5 km thick) ignimbrite and rhyolite unit was formed. This stage is characterized by formation of low-sulfide cassiterite-quartz greisen deposits, spatially associated with Campanian intrusions of leucocratic granites (Gonevchuk, 2002). During this time the unique Dalnegorskoe danburite skarn deposit was formed (Ratkin et al., 2016a,b), along with low-sulfide cassiterite-silicate-sulfide veins in the western part of the subprovince.

The third (final) stage of magmatism took place in Paleocene times (65–57 Ma). When subduction-related activity in the East Sikhote-Alin volcanic belt was terminated due to initiation of the transform-type regime. However, the volcano-plutonic centers retained their spatial association with the structures of the preceding subduction stage, but magmatism was substantially contributed by asthenospheric diapirs (Kazachenko et al., 2013; Grebennikov et al., 2016), breaking through the stagnant slab (Fig. 2c). During this period of magmatism, a dacite-andesite volcanic sequence was formed. Granodiorite and hornblende granite bodies of I-type prevail among the Paleocene intrusions. According to Sr-Nd-Hf isotope data (Jahn et al., 2015), the contamination of granitic melts by upper crust material is estimated at 40–60%.

Metalogenically, the Paleocene was the most productive episode. The Paleocene diorite-granodiorite-granite complexes associate with absolutely all the deposits of lead-zinc veins and skarn ores in the eastern part of the subprovince as well as with numerous cassiterite-silicate-sulfide vein deposits in the western part of the subprovince.

## 3. Ore districts and deposits selected for lead isotope study

### 3.1. Type deposits

Within the SSAP, more than 30 large deposits of Sn, B, Pb and Zn are known. All deposits are located in the Zhuravlevka and Taukha terranes and in overlapping assemblages (Figs. 1, 3–5). Most deposits are tin veins and stockworks. They are located, with few exceptions, in rear zone of the East-Sikhote-Alin volcano-plutonic belt (ESAVB). According Finashin (1986) and Nokleberg (2010) there are three subtypes of mineralization: cassiterite-silicate-sulfide, cassiterite-sulfide and cassiterite-quartz (Sn-W). Pb-Zn deposits are confined to main volcanic zone of the the ESAVB. They can be subdivided into two subtypes: Zn-Pb ( ± Ag, Cu) skarns and Pb-Zn ± Cu ( ± Ag) polymetallic veins (Korsunov, 1995). Borosilicate danburite and datolite skarn deposits are spatially associated with the Zn-Pb skarn deposits (Ratkin et al., 2016b).

For this study we selected 20 deposits located in four large ore districts of SSAP: Dalnegorsk, Krasnorechensk, Kavalerovo and Armin (Table 1, Fig. 1).

### 3.2. The Dalnegorsk district

The Dalnegorsk district is located within the Taukha terrane and in the main zone of the ESAVB in the eastern (coastal) part (Figs. 1 and 3). There are widespread Late Cretaceous-Paleogene magmatic formations in the region. Volcanic rocks of the ESAVB almost entirely overlap the accretionary prism of the Taukha terrane. The deposits mainly comprise Pb-Zn skarn ores of Paleocene age. They are localized above 400–500 m above the granitoid (dioritic, granodioritic, granitic) intrusions of the calc-alkaline series (Korsunov, 1995). The mineralization is associated

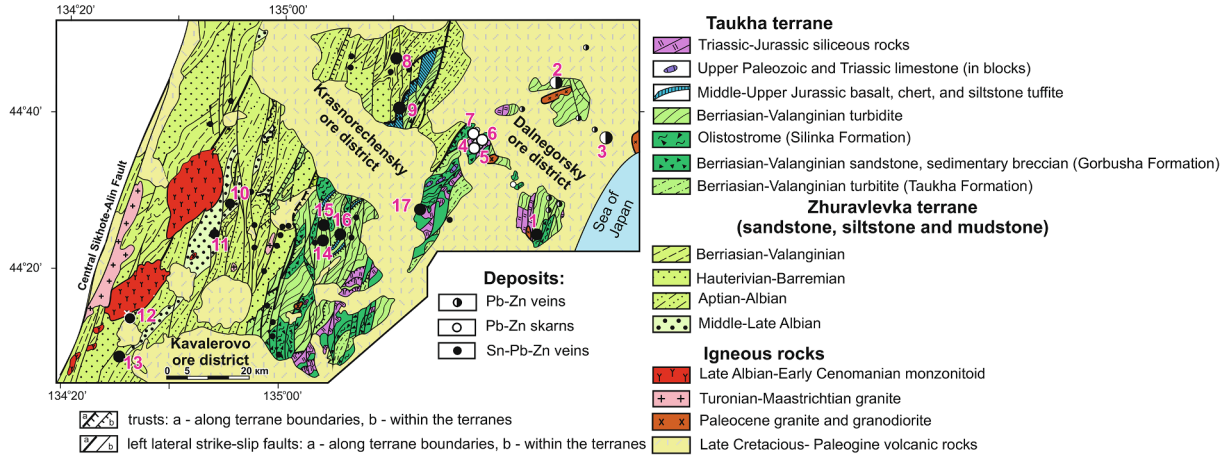


**Fig. 3.** Structural-lithological map of the fold complexes of Kavalerovo, Krasnorechensk and Dalnegorsk districts (modified after Golozoubov, 2006). The numbers shown on the map correspond to the numbers of the deposits in Table 1.

with zones of infiltration. The ilvaite-andradite-hedenbergite skarns were developed at the contacts of Triassic limestone block with sandstones and siltstones in the olistostrome (Ratkin et al., 2016b). The Pb-Zn vein type deposits are subordinate. They spatially associate with the Paleocene volcanic centers, which are located in the sedimentary rocks of the accretionary prism and in the Late Cretaceous volcanic rocks. The vein type deposits, as well as skarns, were formed in the Paleocene.

Among the skarn deposits, we studied the Partizanskoe, Verkhnee, Pervoe Sovetskoe and Dalnegorskoe deposits (Figs. 3 and 4). The latter encompasses two types of skarns, spatially combined in the orebodies: early grossular-wollastonite and danburite(?) and late (Paleocene) ilvaite-andradite-hedenbergite and datolite types (Ratkin et al., 2018). The vein mineralization, for our study, was sampled at the Novomonastyrskoe, Mayminovskoe and Krasnogorskoe deposits. The orebodies of the Novomonastyrskoe and Mayminovskoe deposits are confined to the Triassic-Jurassic and Early Cretaceous sedimentary rocks, respectively, while the Krasnogorskoe deposit is hosted in Late Cretaceous felsic volcanics.

### 3.3. The Krasnorechensk district

The Krasnorechensk district is located in the Zhuravlevka terrane to the west of the Dalnegorsk district, at the boundary between the main and rear zones of the ESAVB (Fig. 1). The sedimentary rocks are dominated by the Early Cretaceous Zhuravlevka complex, mainly occurring in the western and central parts of the district (Fig. 3). In the east, apart from the Early Cretaceous sedimentary rocks are the blocks of Jurassic basalts, cherts, siltstones, and Berriasian-Valanginian sandstones of the Taukha complex. The Late Cretaceous-Paleocene and Eocene volcanic rocks are abundant as well. Early Cenomanian monzodiorite and diorite form small outcrops. Intrusions are surrounded by a wide aureole of biotite hornfels (Valuy and Strizhkova, 1997).

Spatially, the monzodiorite and diorite intrusions are accompanied by the Early Cenomanian cassiterite-sulfide veins in the flysch (Yuzhnoe deposit), and in the areas where flysch associates with Jurassic basalts and cherts (Smirnovskoe deposit). The cassiterite-sulfide ores are dynamically metamorphosed and recrystallized in places where they are

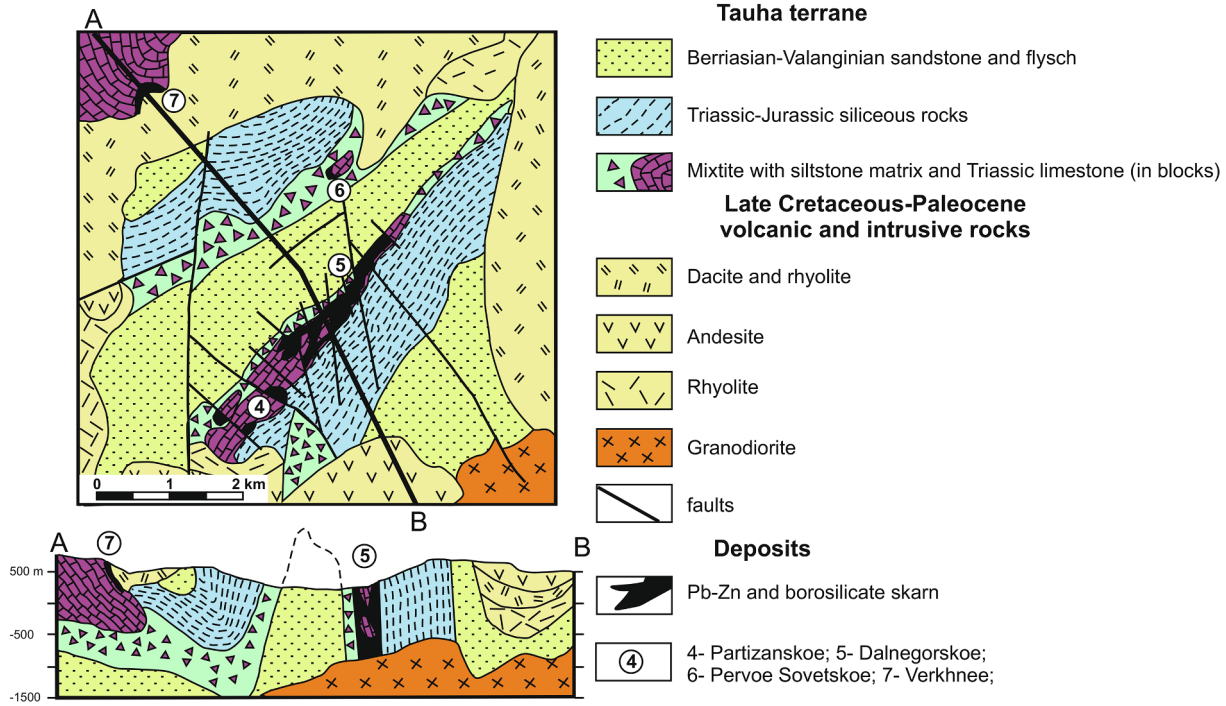


**Fig. 4.** Geological scheme of western part of Dalnegorsk district and cross-section (A-B- line), modified and supplemented after (Golozoubov, 2006).

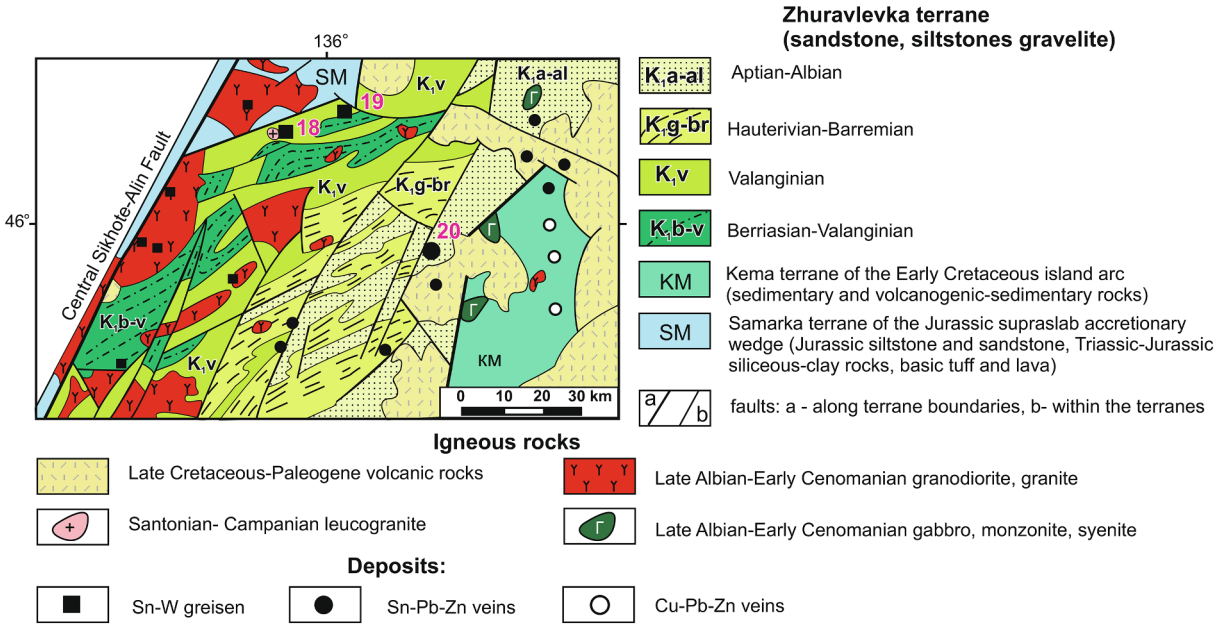


**Fig. 5.** Structural-lithological map of Armin district according to the data of (Bazhanov and Oleynik, 1989) revised and expanded. The numbers shown on the map correspond to the numbers of the deposits in Table 1.

crosscut by greisen veins (cassiterite-quartz ores) of Maastrichtian to Paleocene age. The veins of Yuzhnoe and Smirnovskoe deposits were sampled for lead isotope study.

### 3.4. The Kavalerovo district

The Kavalerovo district is located southwestwards of the Dalnegorsk ore district. The majority of the known tin vein deposits of the SSAP is confined to this area. In the western part of the region (Zhuravlevka terrane), tin deposits are constrained to the Hauterivian-Albian flysch units of the Zhuravlevka complex, while in the east (Taukha terrane) they occur within the Taukha complex (Fig. 3). Igneous rocks mainly occur in the west, represented by the early Cenomanian monzonite and Turonian-Campanian biotite granites (Gonevchuk, 2002; Kruk et al., 2019). The Maastrichtian to Paleocene magmatic formations in this area form small granite-granodiorite bodies and dyke swarms.

In this area, we studied deposits from both the western (Sobolinoe-I, Novogorskoye, Arsenyevskoe, Iskra (western group)) and eastern part (Khrustalnoe, Verkhnezinkovoye, Silinskoe and Vysokogorskoe (eastern group)). The western group deposits, despite their similar geological position, differ from each other in a number of characteristics. The oldest deposits are assumed to be the Sobolinoe-I and Novogorskoe, where the mineralization is genetically associated with post-accretionary Cenomanian (95–90 Ma) magmatic rocks (Gonevchuk et al., 2011). These deposits differ in their mineral composition and content of the main ore components. At the Sobolinoe-I deposit, cassiterite-antimony-lead ores form low angle vein bodies, hosted by chlorite alteration, whereas the Novogorskoe cassiterite-sulfide ores spatially associate with a granodiorite stock.

At the Arsenyevskoe deposit, the largest reserve in the Kavalerovo district, ore bodies of two ages are spatially combined. The cassiterite-sulfide west-east-trending veins, occurring in the tourmalinites, are considered to be the earliest (Early Cenomanian). They are genetically related to the monzonite and granodiorite intrusions (Finashin, 1986; Tomson et al., 1996; Gonevchuk et al., 2011). The younger cassiterite-silicate-sulfide ores form veins, cross-cutting the tourmalinites. The younger ores are spatially and temporally related to rhyolite and andesite dykes. The dykes demonstrate their formation with participation of a fluid-magmatic phase, derived from the residual melt of a magma chamber (Nekrasov and Popov, 1990). The age of ores is estimated at 60–55 Ma (Gonevchuk, 2002) by analogy with an age of the intra-ore dykes. The Pb isotopic composition was studied in galena from the early and younger ores. The youngest cassiterite-silicate-sulphidesulfide ores (Iskra deposit) are assumed to be 63–61 Ma in age (Gonevchuk et al., 2005).

The deposits of the eastern group are located within the Taukha accretionary prism. These are vein-type deposits with cassiterite-silicate-sulfide (Khrustalnoe, Vysokogorskoe) and cassiterite-sulfide (Verkhnezinkovoe, Silinskoe) mineralization. It is assumed that their formation took place in two stages. During the early (Cenomanian-Turonian) stage, the orebodies with cassiterite-sulfide mineralization were formed. They are spatially associated with the Late Cretaceous granitoid intrusions. Younger orebodies (cassiterite-silicate-sulfide veins) within the fluid-explosive breccia are genetically related to the Paleocene complex of intra-ore dykes of quartz porphyry and plagioclase-bearing felsite (Radkevich et al., 1980; Tomson et al., 1996; Kokorin et al., 2001).

### 3.5. The Armin district

The Armin district is located north of Kavalerovo district within the Zhuravlevka terrane and in the back rear zone of the ESAVB (Fig. 1). The deposits are hosted by the Early Cretaceous complexes of the Zhuravlevka terrane (Fig. 5), intruded by numerous large late Albian to early Cenomanian granitoid plutons (Kruk et al., 2019). Small Li-F-leucogranite intrusions of the Santonian-Campanian age occur in the western part of the region at the boundary with the Samarka terrane (Fig. 5). Mineralization is mainly represented by the cassiterite-sulfide vein-type. The mineralization is associated with the Late Cretaceous monzodiorite intrusions (Finashin, 1986). Tin-tungsten greisen deposits associate with the Li-F-leucogranite intrusions. The age of the intrusion and greisen formation, according to Rb-Sr dating, is ca. 80 Ma (Belyatsky et al., 1994).

In the present work, the Ternistoe (cassiterite-sulfide vein-type), Tigrinoe and Tabornoe (Sn-W greisen type) deposits have been studied (Table 1).

**Table 1**
Geological and mineralogical characteristics of the studied deposits of SSAP (Russian Far East) (Gonevchuk, 2002; Gonevchuk et al., 2005, 2011; Tomson et al, 1996; Finashin, 1986; Nekrasov and Popov, 1990).

| N | Deposit | Host rocks | Ore type | Age (Ma) | Mineralogy | | Number of samples |
|---|---|---|---|---|---|---|---|
| | | | | | gangue minerals | ore minerals | |
| *Dalnegorsk district* | | | | | | | |
| Taukha terrane | | | | | | | |
| 1 | Novomonastyrskoe | sandstones ($K_1$) + cherts (T-J) | cassiterite-sulfide veins | 90–95 | q, chl, tur | cs, cp, py, sl | 1 |
| 2 | Maiminovskoe | sandstones ($K_1$) | polymetallic veins (Pb-Zn ± Cu( ± Ag)) | 60–65 | chl, q | cs, pyr, sl, gn | 1 |
| 3 | Krasnogorskoe | ignimbrites ($K_2$) | polymetallic veins (Pb-Zn ± Cu( ± Ag)) | 60–65 | q, cal, chl, ort, ser | sl, gn, cp, py, apy, Ag-ss | 1 |
| 4 | Partizanskoe | sandstones ($K_1$) + limestone + cherts (T-J) | Zn-Pb skarn | 57–60 | q, cal, chl, ser | sl, gn, cp, py, apy, Ag-ss | 1 |
| 5 | Dalnegorskoe | sandstones ($K_1$) + limestones + cherts (T-J) | B skarn (dunburite) | 78 | wol, gr, q | db ( ± sl, gn) | 1 |
| | | | B skarn (datolite) | 57 | hed, and, il, ort, q, cal | dt, ak, sl, gn | 1 |
| 6 | Pervoe Sovetskoe | sandstones ($K_1$) + limestone + cherts (T-J) | Zn-Pb skarn | 57–60 | hed, and, il, q, cal | sl, gn, cp, py, apy, mt, fr | 1 |
| 7 | Verkhnee | sandstones ($K_1$) + limestone + cherts (T-J) | Zn-Pb skarn | 57–60 | hed, and, il, q, cal | sl, gn, cp, py, apy, mt, fr | 2 |
| *Krasnorechensk district* | | | | | | | |
| Zhuravlevka terrane | | | | | | | |
| 8 | Yuzhnoe | sandstones ($K_1$) | cassiterite -sulfide veins | 90-95 | chl, ser, q | cs, apy, pyr, sl, gn, sn, Ag-ss, bi | 8 |
| Taukha terrane | | | | | | | |
| 9 | Smirnovskoe | sandstones ($K_1$) + basalts, cherts ($J_{2-3}$) | cassiterite -sulfide veins | 90–95 | chl, ser, q | cs, apy, pyr, sl, gn, sn, Ag-ss, bi | 2 |
| *Kavalerovo district* | | | | | | | |
| Zhuravlevka terrane | | | | | | | |
| 10 | Arsenievskoe | sandstones ($K_1$) | cassiterite -sulfide veins | 90–70 | tur | cs, sl, gn, mt, cp, apy, pyr, sn | 2 |
| | | | cassiterite -silicate-sulfide veins | 60–55 | q, cal | cs, sl, gn | 12 |
| 11 | Novogorskoe | sandstones ($K_1$) | cassiterite -sulfide veins | 90–95 | chl, tur | cs, apy, pyr, sl, gn | 1 |
| 12 | Iskra | sandstones ($K_1$) | cassiterite -silicate-sulfide veins | 61–63 | q, chl | cs, cp, sl, gn | 1 |
| 13 | Sobolinoe-I | sandstones ($K_1$) | cassiterite-sulfide veins | 90–95 | chl | cs, gn, bl, Ag-ss, fr | 2 |
| *Kavalerovo district* | | | | | | | |
| Taukha terrane | | | | | | | |
| 14 | Khrustalnoe | sandstones ($K_1$) + cherts ($J_{2-3}$) | cassiterite -silicate-sulfide veins | 65 ± 3 | q, chl, ser | cs, sl, gn, pyr | 1 |
| 15 | Verkhnezinkovoe | sandstones ($K_1$) + cherts ($J_{2-3}$) | cassiterite -sulfide veins | 90–95 | chl, tur | cs, pyr, sl, gn | 1 |
| 16 | Silinskoe | cherts ($J_{2-3}$) + sandstones ($K_1$) | cassiterite-sulfide veins | 80 ± 3 | chl, q | cs, sl, pyr, apy, cp, py, st | |
| | | | cassiterite-silicate-sulfide veins | 56 ± 2 | q, chl, mus | cs, apy, sl, gn | 4 |
| 17 | Vysokogorskoe | cherts (T-J) + sandstones ($K_1$) | cassiterite-silicate-sulfide veins | 60 | q, chl, tur | cs, cp, py, sl | 2 |
| *Armin district* | | | | | | | |
| Zhuravlevka terrane | | | | | | | |
| 18 | Tigrinoe | sandstones ($K_1$) | Sn-W greisen veins | 80 | q, top, zin, ort | cs, wl, sh, mo, py, cp, sl, gn | 1 |
| 19 | Tabornoe | sandstones ($K_1$) | Sn-W greisen veins | 80 | q, top, zin, ort | cs, wl, sh, mo, py, cp, sl, gn | 1 |
| 20 | Ternistoe | sandstones ($K_1$) | cassiterite -sulfide veins | 90–95 | tur,chl, ser, q | cs, cp, apy, pyr, sl, gn, mt | 1 |

cs – cassiterite, gn – galena, sl – sphalerite, cp – chalcopyrite, bl – boulangerite, Ag-sulfosalts, fr – freibergite, pyr – pyrrhotite, py – pyrite, sn – stannite, apy – arsenopyrite, wl – wolframite, mt – magnetite, q – quartz, chl – chlorite, tur – tourmaline, cal – calcite, il – ilvaite, an – andradite, hd – hedenbergite, gr – grossular, wol – wollastonite, db – danburite, dat – datolite, ak – axinite, top – topaz, zin – zinnwaldite, ort – orthoclase, ser – sericite, bi – bismuth minerals, mo – molybdenite, sh – scheelite, mus – muscovite.

## 4. Sampling, sample preparation and analytical techniques

### 4.1. Sampling

Three suites of samples were studied. These are: (1) 48 galena samples from 20 deposits; (2) seven samples of fresh feldspar from the Late Cretaceous-Paleocene granitoids; (3) ten whole rock samples from the Early Cretaceous sedimentary rocks of the Taukha and Zhuravlevka terranes.

Most of the studied deposits are confined to the two metallogenic districts: Kavalerovo (8 deposits) and Dalnegorsk (7 deposits). In other districts – Armin and Krasnorechensk, – three and two deposits respectively have been studied. Each deposit is characterized by one or two galena samples. The most detailed data were obtained for the two large tin deposits: Yuzhnoe cassiterite-sulfide and Arsenyevskoe cassiterite-silicate-sulfide.

The feldspar samples were collected from granitoids of the Kavalerovo and Dalnegorsk districts. In the Kavalerovo district, the Late Cretaceous (ca. 75 Ma; Jahn et al., 2015) main phase granite and pegmatite of the Shumnensky massif were sampled. Also, granitic debris from ore-bearing explosive breccia at the Arsenievskoe deposit have been studied. In the Dalnegorsk district, the Paleocene (ca. 60 Ma; Alenicheva and Sakhno, 2008) granites of Dalnegorsk and Klyuch-27 massifs have been studied.

**Table 2**
Lead isotopic composition of galena in deposits of the South Sikhote-Alin subprovince (Russian Far East).

| N | Sample | Deposit | $^{206}Pb/^{204}Pb$ | $^{207}Pb/^{204}Pb$ | $^{208}Pb/^{204}Pb$ | Tм (Ma) | $\mu_2$ | $\omega_2$ | Th/U |
|---|---|---|---|---|---|---|---|---|---|
| *Dalnegorsk district* | | | | | | | | | |
| 1 | Ui-240–01 | Novomonastyrskoe | 18.4507 | 15.6553 | 38.7591 | 246 | 9.91 | 39.9 | 4.03 |
| 2 | Ui-235–01 | Maiminovskoe | 18.3524 | 15.6214 | 38.6343 | 250 | 9.79 | 39.3 | 4.01 |
| 3 | Sh-1 | Krasnogorskoe | 18.3917 | 15.6163 | 38.6014 | 209 | 9.75 | 38.7 | 3.97 |
| 4 | 81 | Partizanskoe | 18.3870 | 15.6276 | 38.6745 | 236 | 9.80 | 39.4 | 4.02 |
| 5 | 336–1-2 | Dalnegorskoe (late mineral assemblage in skarns) | 18.3864 | 15.6189 | 38.6360 | 219 | 9.77 | 39.0 | 3.99 |
| 6 | 337–2 | Dalnegorskoe (early mineral assemblage in skarns)) | 18.3904 | 15.6207 | 38.6471 | 220 | 9.77 | 39.0 | 4.00 |
| 7 | 98 | Pervoe Sovetskoe | 18.3861 | 15.6261 | 38.6691 | 234 | 9.80 | 39.3 | 4.01 |
| 8 | 62 | Verkhnee | 18.3865 | 15.6270 | 38.6728 | 236 | 9.80 | 39.4 | 4.02 |
| 9 | 343-1b | same | 18.3894 | 15.6282 | 38.6661 | 236 | 9.81 | 39.3 | 4.01 |
| *Krasnorechensk district* | | | | | | | | | |
| 10 | 213–2001 | Yuzhnoe, vein N 4, level 850 | 18.3288 | 15.6219 | 38.6624 | 268 | 9.79 | 39.6 | 4.05 |
| 11 | 238–2001 | same, level 760 | 18.3294 | 15.6238 | 38.6687 | 272 | 9.80 | 39.7 | 4.05 |
| 12 | 235–2001 | same, level 550 | 18.3265 | 15.6214 | 38.6603 | 269 | 9.79 | 39.6 | 4.05 |
| 13 | U-2 | same, east edge | 18.3231 | 15.6231 | 38.6627 | 275 | 9.80 | 39.7 | 4.05 |
| 14 | U-3 | same | 18.3223 | 15.6222 | 38.6593 | 274 | 9.80 | 39.7 | 4.05 |
| 15 | U-4 | same, west edge | 18.3234 | 15.6237 | 38.6644 | 276 | 9.80 | 39.7 | 4.05 |
| 16 | U-10 | same | 18.3228 | 15.624 | 38.6650 | 277 | 9.81 | 39.7 | 4.05 |
| 17 | U-11 | same | 18.3209 | 15.6224 | 38.6656 | 275 | 9.80 | 39.7 | 4.05 |
| 18 | K-10 g | Smirnovskoe | 18.3208 | 15.6237 | 38.6672 | 278 | 9.80 | 39.8 | 4.06 |
| 19 | 67 | same | 18.3602 | 15.6285 | 38.6864 | 258 | 9.82 | 39.7 | 4.04 |
| *Kavalerovo district* | | | | | | | | | |
| 20 | 155–86 | Arsenievskoe, vein Fevralskay, level IV, late mineral assemblage | 18.4057 | 15.611 | 38.6358 | 188 | 9.73 | 38.7 | 3.97 |
| 21 | 156–86 | same | 18.4027 | 15.6082 | 38.6263 | 184 | 9.72 | 38.6 | 3.97 |
| 22 | 237–86 | Arsenievskoe, vein Fevralskay, level X, late mineral assemblage | 18.4036 | 15.6088 | 38.6285 | 185 | 9.72 | 38.6 | 3.97 |
| 23 | 241–86 | same | 18.4047 | 15.6103 | 38.6357 | 187 | 9.72 | 38.7 | 3.98 |
| 24 | 254–86 | same | 18.4039 | 15.6085 | 38.6264 | 184 | 9.72 | 38.6 | 3.97 |
| 25 | 255–86 | same | 18.4041 | 15.6092 | 38.6284 | 185 | 9.72 | 38.6 | 3.97 |
| 26 | 359–86 | Arsenievskoe, vein Yuznay, level IV, late mineral assemblage | 18.4037 | 15.6091 | 38.6305 | 185 | 9.72 | 38.6 | 3.97 |
| 27 | 57–88 | same, level VII, late mineral assemblage | 18.4039 | 15.6109 | 38.6352 | 189 | 9.73 | 38.7 | 3.97 |
| 28 | 382–86 | same, level VIII, late mineral assemblage | 18.4036 | 15.6091 | 38.6288 | 185 | 9.72 | 38.6 | 3.97 |
| 29 | 361–86 | Arsenievskoe, vein Glavnay, level VII, late mineral assemblage | 18.4031 | 15.6083 | 38.6267 | 184 | 9.72 | 38.6 | 3.97 |
| 30 | 241–87 | Arsenievskoe, vein Turmalinovay, level VIII, early mineral assemblage | 18.4051 | 15.6086 | 38.629 | 183 | 9.72 | 38.6 | 3.97 |
| 31 | 93–87 | same, level IX, early mineral assemblage | 18.4047 | 15.6095 | 38.6200 | 185 | 9.72 | 38.6 | 3.97 |
| *Kavalerovo district* | | | | | | | | | |
| 32 | 7723 | Arsenievskoe, vein Indukcionnay, level IV, late mineral assemblage | 18.4054 | 15.6105 | 38.6337 | 187 | 9.72 | 38.6 | 3.98 |
| 33 | 430–88 | same, level X, late mineral assemblage | 18.4029 | 15.6094 | 38.6270 | 187 | 9.72 | 38.6 | 3.97 |
| 34 | K-105–2004 | Novogorskoe | 18.4024 | 15.6148 | 38.6198 | 198 | 9.74 | 38.7 | 3.97 |
| 35 | 121–2000 | Iskra | 18.3985 | 15.6158 | 38.6387 | 203 | 9.75 | 38.8 | 3.98 |
| 36 | GV-977 | Sobolinoe-I | 18.3948 | 15.6135 | 38.6320 | 201 | 9.74 | 38.8 | 3.98 |
| 37 | 150–2001 | same | 18.3961 | 15.6158 | 38.6395 | 205 | 9.75 | 38.9 | 3.99 |
| 38 | 171 | Khrustalnoe | 18.4093 | 15.6137 | 38.6417 | 191 | 9.74 | 38.7 | 3.98 |
| 39 | 13 | Verkhnezinkovoe | 18.4174 | 15.6391 | 38.7681 | 237 | 9.85 | 39.9 | 4.05 |
| 40 | 1-Б | Silinskoe | 18.4214 | 15.6419 | 38.7874 | 240 | 9.86 | 40.0 | 4.06 |
| 41 | 142 | same | 18.4221 | 15.6435 | 38.7959 | 243 | 9.87 | 40.1 | 4.06 |
| 42 | 368 | same | 18.4184 | 15.6356 | 38.7538 | 229 | 9.83 | 39.7 | 4.04 |
| 43 | 370–2 | same | 18.4185 | 15.6348 | 38.7487 | 228 | 9.83 | 39.7 | 4.04 |
| 44 | GVC-1 | Vysokogorskoe | 18.4741 | 15.6519 | 38.7776 | 221 | 9.89 | 39.7 | 4.02 |
| 45 | Ui-229 | same | 18.4520 | 15.6420 | 38.7360 | 217 | 9.85 | 39.5 | 4.01 |
| *Armin district* | | | | | | | | | |
| 46 | 1063 | Tigrinoe | 18.4201 | 15.6327 | 38.6745 | 222 | 9.82 | 39.2 | 3.99 |
| 47 | 1007 | Tabornoe | 18.4223 | 15.6358 | 38.6844 | 227 | 9.83 | 39.3 | 4.00 |
| 48 | 284–78 | Ternistoe | 18.3861 | 15.6262 | 38.6708 | 234 | 9.80 | 39.3 | 4.01 |

Analytical error for Pb isotope ratios in galena is ± 0.02% (2SD).

The sedimentary rock samples are from Early Cretaceous complexes of the Taukha and Zhuralevka terranes. Two of the studied sandstone and siltstone samples are from the Dalnegorsk district, another two samples are from the Armin district, and six more are from the Kavalerovo district.

### 4.2. Lead isotopic analysis

The authors analyzed Pb isotope composition at the IGEM RAS using the high-precision MC-ICP-MS method from solutions spiked by thallium with a known $^{205}Tl/^{203}Tl$ isotopic ratio to correct the results for instrumental mass-bias.

#### 4.2.1. Chemical preparation

For the Pb isotope analysis, one thoroughly selected grain of galena weighing 0.001–0.003 g was dissolved in a droplet of 70% $HNO_3$. In case of sedimentary rock (siltstone, sandstone) analysis, 0.08–0.1 g of the whole rock powder was taken. For the feldspar analysis, 0.05–0.08 g of 0.5–0.25 mm selected grains were utilized. In order to remove possible Pb contamination from grain surface, feldspar fractions were pretreated with 10% $HNO_3$ for 2 h at 90° C. Chemical digestion procedure of the whole rock samples and feldspar samples was the same. Samples were dissolved in a $HNO_3$ + HF (1: 3) mixture for two days at 140 °C. Subsequently, the solution was evaporated to dry salts. Separation of Pb from major and trace rock elements was carried out employing a one-step scheme with HBr medium in a chromatographic

microcolumn (0.1 $cm^3$) filled with anion exchange resin AG-1 × 8 (Chugaev et al., 2013b). The laboratory blank contribution for Pb is about 0.1 ng.

#### 4.2.2. Mass spectrometry measurements of Pb isotopes

The Pb isotope composition measurements in the samples were carried out with method proposed by Rehkämper and Halliday (1998) applying NEPTUNE multi-collector mass-spectrometer (Thermo-Finnigan, Germany). Details of the analytical procedure were described in Chernyshev et al. (2007). Chemically separated Pb fractions were analyzed in a 3% $HNO_3$ solution in a "wet" plasma mode. Lead concentrations in the solutions were 100–400 ng/ml, which ensured a $^{208}Pb^+$ ion current of 1.5–8 × $10^{-11}$ A. Just before the measurements, the sample solutions were doped by Tl-spike, in which $^{205}Tl/^{203}Tl$ value is equal 2.3889 ± 1. Mass-bias correction for the measured Pb isotope ratios was performed using the reference ratio $^{205}Tl/^{203}Tl$ employing an exponential law. Precision and accuracy of the results were monitored by systematic analyses of the SRM 981 and reference andesite sample AGV-2 (USGS). In a series of parallel analyses, average value of Pb isotope ratios were: for SRM 981 – $^{206}Pb/^{204}Pb$ = 16.940 ± 3; $^{207}Pb/^{204}Pb$ = 15.499 ± 3; $^{208}Pb/^{204}Pb$ = 36.723 ± 7, (n = 28); for AGV-2 – $^{206}Pb/^{204}Pb$ = 18.871 ± 4; $^{207}Pb/^{204}Pb$ = 15.621 ± 2; $^{208}Pb/^{204}Pb$ = 38.548 ± 6 (n = 9). Based on these results, a total error ( ± 2SD) of Pb isotopic composition in galena is assumed to be ± 0.02%. For feldspar and sedimentary rock samples the total error did not exceed ± 0.03%.

### 4.3. U, Th, Pb concentration analyses by ICP-MS method

To estimate the initial Pb isotope composition in the sedimentary rocks and feldspars, Pb, Th, and U concentrations have been determined in the same samples as for Pb isotope composition. The analyses were carried out on X-7 ICP-MS quadrupole mass spectrometer (Thermo Elemental) in solutions of samples doped with indium. The accuracy of elemental analysis, assessed by results of systematic measurements of standard rock samples BHVO-2 and AGV-2, did not exceed ± 3% ( ± 2SD).

The obtained data on the Pb, Th, and U contents were used to correct the measured lead isotope ratios for radiogenic $^{206}Pb$, $^{207}Pb$, and $^{208}Pb$ accumulated in the granite feldspar and sedimentary rock samples as a result of *in situ* radioactive decay of U and Th. The feldspar data are corrected for the ages of granite intrusions. The sedimentary rock data were corrected for 90 and 60 Ma, corresponding to the ages of the SSAP main ore epochs (Table 1).

## 5. Results

Results of Pb isotopic determinations in galena from the SSAP deposits are listed in Table 2. The Pb-Pb data obtained from the sedimentary rock samples and feldspar fractions from granitoids, spatially associated with the deposits, are given in Table 3.

### 5.1. Pb isotopic composition of galena

In general, Pb isotope ratios in galena vary within narrow limits: $^{206}Pb/^{204}Pb$ ranges from 18.321 to 18.474; $^{207}Pb/^{204}Pb$ – 15.608–15.655; and $^{208}Pb/^{204}Pb$ 38.601–38.796; i.e. the marginal values differ in 0.8, 0.3, and 0.5%, respectively. Evidently, these differences exceed the errors of the analytical technique applied ( ± 0.02%, 2SD) by more than an order of magnitude.

The most comprehensive data were obtained for the Kavalerovo and Dalnegorsk ore districts (Table 2). Spatially, these areas are close, but differ in their geological structure. The Kavalerovo district overlaps the Zhuravlevka and Taukha terranes, while the Dalnegorsk district is entirely located within the latter terrane. Comparison of the districts shows that they are similar in galena Pb isotope composition and are equally homogenous: $^{206}Pb/^{204}Pb$ (18.35–18.47), $^{207}Pb/^{204}Pb$ (15.61–15.66), and $^{208}Pb/^{204}Pb$ (38.60–38.80). The Armin district is also similar to the former two ($^{206}Pb/^{204}Pb$ = 18.39–18.42, $^{207}Pb/^{204}Pb$ = 15.63–15.64, $^{208}Pb/^{204}Pb$ = 38.67–38.68), despite the deposits are located about 200 km northwards of the Kavalerovo district. In isotope diagrams (Fig. 6a, b), lead isotope signature fields of the districts overlap. The Pb isotope ratios of galena from Krasnorechensk district, neighboring the Dalnegorsk district from the west, also range with in narrow limits: $^{206}Pb/^{204}Pb$ from 18.32 to 18.36; $^{207}Pb/^{204}Pb$ from 15.621 to 15.629; and $^{208}Pb/^{204}Pb$ from 38.60 to 38.69. There is a small but notable difference in $^{206}Pb$ radiogenic isotope content between the deposits of Krasnorechensky district and that of other SSAP districts. This results in clear distinction of the Krasnorechensky district average $^{206}Pb/^{204}Pb$ = 18.33 ± 0.01 (SD) from that of the other districts (Kavalerovo – $^{206}Pb/^{204}Pb$ = 18.41 ± 0.02, Dalnegorsk – $^{206}Pb/^{204}Pb$ = 18.39 ± 0.03, Armin – $^{206}Pb/^{204}Pb$ = 18.41 ± 0.02). In the Pb-Pb diagrams, the field of the Krasnorechensk district shift to the left and does not overlap with the other SSAP districts (Fig. 6a, b).

### 5.2. Pb isotope composition of the granite feldspars and bulk sedimentary rocks

The measured lead isotope ratios in feldspars show rather narrow ranges when compared with the SSAP deposits. The $^{206}Pb/^{204}Pb$, $^{207}Pb/^{204}Pb$ and $^{208}Pb/^{204}Pb$ ratios range: from 18.41 to 18.49, from 15.61 to 15.63 and from 38.61 to 38.74, respectively (Table 3). In most feldspar samples, the U/Pb and Th/Pb ratios are low and do not exceed 0.04 and 0.15, respectively. One exception is the sample V-1575, in which U/Pb and Th/Pb are higher (0.14 and 0.44). The age-corrected lead isotopic ratios differ little from the measured signatures. The age-corrected $^{206}Pb/^{204}Pb$ (or $(^{206}Pb/^{204}Pb)_t$) ratio varies from 18.40 to 18.43, $(^{207}Pb/^{204}Pb)_t$ from 15.61 to 15.63, and $(^{208}Pb/^{204}Pb)_t$ from 38.61 to 38.70. The sample V-1575 shows the maximum differences between the measured and age-corrected $^{206}Pb/^{204}Pb$ ($\Delta$ = 0.45%) and $^{208}Pb/^{204}Pb$ ($\Delta$ = 0.2%) ratios. These differences are 3 or more times smaller in the case of other feldspar samples.

The whole rock sedimentary samples show higher values of U/Pb (0.09–0.53) and Th/Pb (0.6–3.1) ratios in comparison with the feldspar samples. The measured Pb isotope ratios range within wider limits when compared with the SSAP deposits and granite feldspar samples: $^{206}Pb/^{204}Pb$ varies from 18.29 to 18.86; $^{207}Pb/^{204}Pb$ from 15.60 to 15.66; and $^{208}Pb/^{204}Pb$ from 38.54 to 39.31 (Table 3). After age correction, the limits change, but still remain wide. For the age of 90 Ma, $(^{206}Pb/^{204}Pb)_t$ ratio ranges from 18.19 to 18.58, $(^{207}Pb/^{204}Pb)_t$ from 15.59 to 15.66, and $(^{208}Pb/^{204}Pb)_t$ from 38.33 to 38.90. For the age of 60 Ma, $(^{206}Pb/^{204}Pb)_t$ ratio ranges from 18.22 to 18.64, $(^{207}Pb/^{204}Pb)_t$ from 15.59 to 15.66, and $(^{208}Pb/^{204}Pb)_t$ from 38.40 to 38.99.

The following discussion is based only on the age-corrected lead isotopic ratios.

## 6. Discussion

### 6.1. Lead isotope systematics of SSAP deposits

A scale of variations of Pb isotope composition is an important geochemical characteristics of a metallogenic province. Traditionally, it is estimated by a variation coefficient ($\nu$,%) (Gulson, 1986). For SSAP deposits, differing by the mineralization type and scale, the variation coefficients are relatively small: $\nu_{6/4}$ = 0.2%, $\nu_{7/4}$ = 0.08% and $\nu_{8/4}$ = 0.13%. By this parameter, the SSAP can be contrastingly distinguished from a number of well-known metallogenic provinces, where deposits (as the case of the SSAP), are genetically associated with magmatism. For example, the Pb isotope variation coefficient for the Central Andes, Eastern Transbaikalia (Russia) and Iran, having representative Pb-Pb data, are several times larger and constrained to: $\nu_{6/4}$ from 0.8 to 2.0%, $\nu_{7/4}$ from 0.18 to 0.30% and $\nu_{8/4}$ from 0.3 to 0.9%

**Table 3**
Lead isotopic composition in feldspars of Late Cretaceous-Paleocene granitoids and in Early Cretaceous sedimentary rocks of Taukha and Zhuravlevka terranes (Russian Far East).

| № | Sample | Sample description | Pb, ppm | Th, ppm | U, ppm | $^{206}Pb/^{204}Pb$ | $^{207}Pb/^{204}Pb$ | $^{208}Pb/^{204}Pb$ |
|---|---|---|---|---|---|---|---|---|
| *Late Cretaceous-Paleocene granitoids* | | | | | | | | |
| Kavalerovo district | | | | | | | | |
| 1 | GV-725 | K-feldspar, granite, Shumnensky massif | 24.4 | 2.47 | 0.82 | 18.4596 | 15.6094 | 38.6354 |
| 2 | GV-725-P | K-feldspar, pegmatite, Shumnensky massif | 55.6 | < 0.05 | 0.04 | 18.4099 | 15.6079 | 38.6050 |
| 3 | F-899/6 | feldspars, granitic fragments in the ore-bearing explosive breccia, Arsenievskoe deposit | 41.8 | 3.00 | 0.79 | 18.4144 | 15.6103 | 38.6280 |
| *Dalnegorsk district* | | | | | | | | |
| 4 | V-1575 | feldspars, granite, Klyuch-27 intrusion | 3.79 | 1.67 | 0.52 | 18.4891 | 15.6285 | 38.7378 |
| 5 | V-1499 k | K-feldspar, granite, Dalnegorsky intrusion, | 17.4 | 1.01 | 0.30 | 18.4345 | 15.6296 | 38.6915 |
| 6 | V-1498i | K-feldspar, adamelite, Dalnegorsky intrusion | 14.7 | 1.42 | 0.43 | 18.4508 | 15.6280 | 38.7152 |
| 7 | B-1497–4 | K-feldspar, granite, Dalnegorsky intrusion | 17.4 | 2.57 | 0.72 | 18.4271 | 15.6261 | 38.6937 |
| *Early Cretaceous sedimentary rocks of Taukha terrane* | | | | | | | | |
| Dalnegorsk district | | | | | | | | |
| 8 | 309/1 | Berriasian -Valanginian sandstone | 13.6 | 13.2 | 1.5 | 18.2899 | 15.6614 | 38.9725 |
| 9 | 309/2 | Berriasian -Valanginian sandstone | 16.4 | 11.9 | 1.5 | 18.3123 | 15.6554 | 38.8126 |
| *Early Cretaceous sedimentary rocks of Zhuravlevka terrane* | | | | | | | | |
| Armin district | | | | | | | | |
| 10 | Zh-11 | Early Berriasian- late Valanginian siltstone | 11.8 | 8.35 | 1.88 | 18.5115 | 15.5971 | 38.5422 |
| 11 | Zh-25 | Early Berriasian- late Valanginian siltstone | 5.59 | 17.51 | 2.99 | 18.8588 | 15.6464 | 39.3088 |
| Kavalerovo district | | | | | | | | |
| 12 | Zh-44 | Valanginian siltstone | 14.7 | 17.7 | 3.3 | 18.6803 | 15.6553 | 39.1458 |
| 13 | Zh-48 | Valanginian siltstone | 26 | 16 | 2.9 | 18.4753 | 15.6280 | 38.8145 |
| 14 | Zh-70 | Early-Middle Albian sandstone | 17.2 | 15.8 | 3.1 | 18.7464 | 15.6474 | 39.1703 |
| 15 | Zh-71 | Early-Middle Albian sandstone | 16.6 | 14.9 | 2.8 | 18.5024 | 15.6219 | 38.8370 |
| 16 | Zh-87 | Middle-Late Albian siltstone | 15.1 | 13.8 | 2.7 | 18.5241 | 15.6307 | 38.9394 |
| 17 | Zh-88 | Middle-Late Albian siltstone | 19.1 | 15.3 | 2.8 | 18.5297 | 15.6301 | 38.9511 |

Analytical error for Pb isotope ratios in feldspars and sedimentary rocks is ± 0.03% (2SD). Pb, Th, and U concentrations determined by ICP-MS method in IGEM RAS. The error of elemental analysis did not exceed ± 3% (2SD).

(Macfarlane et al., 1990, Kamenov et al., 2002; Shafiei, 2010; Mirnejad et al., 2011; Chugaev et al., 2013a).

Thus, the SSAP is characterized by a fairly high degree of homogeneity of the ore lead isotope composition. This allows us to conclude that the dominating lead source (geochemical reservoir) for all the studied deposits has a regional extent. This is supported by the fact that the Pb isotope composition of the deposits neither correlate with mineralization type nor with age.

Despite the fact that the whole variation values of the Pb isotope composition in the SSAP is very narrow, subtle differences in the Pb – Pb characteristics were revealed between the deposits within individual districts. This is most clearly exemplified by the Kavalerovo cassiterite-sulfide deposits. Two groups of the deposits can be distinguished there. The variations of $^{207}Pb/^{204}Pb$ and $^{208}Pb/^{204}Pb$ within each of them is 2–3 times lesser than for the entire region and is close to the value of the analytical error. The first group includes the Verkhnezinkovoye, Silinskoe and Vysokogorskoe deposits. They have relatively elevated ratios of $^{207}Pb/^{204}Pb$ (ca. 15.64) and $^{208}Pb/^{204}Pb$ (ca. 38.77) (Fig. 6). On the contrary, the lead in the Arsenyevskoe, Novogorskoe, Iskra, Sobolinoye-I and Khrustalnoe deposits, forming the second group, demonstrate a lower content of $^{207}Pb$ ($^{207}Pb/^{204}Pb$ ca. 15.61) and $^{208}Pb$ ($^{208}Pb/^{204}Pb$ ca. 38.63) (Fig. 6). These differences in the Pb isotopic composition correlate with the deposit's locations within the ore district. The deposits of the first group occur in the east of the district, where volcanics and sedimentory rocks of the Taukha complex are represented. The second group deposits (except for the Khrustalnoe deposit), on the contrary, are confined to the western part. These deposits are hosted by the Early Cretaceous Zhuravlevka flysch. The Khrustalnoe deposit is located in the central part of the region, where the Taukha complex is thrust over the siliciclastic rocks of the Zhuravlevka complex (Golozoubov, 2006).

In the Dalnegorsk district, most of the studied deposits are similar in lead isotopic composition. The variations of Pb isotope ratios detected here are not correlated with the deposit's structural position or their host rock composition. An exception is the Novomonastyrskoe cassiterite-sulfide deposit, which in terms of Pb isotopes differs from the other Dalnegorsk deposits: it has a polymetallic type of mineralization. In terms of the $^{207}Pb/^{204}Pb$ and $^{208}Pb/^{204}Pb$ ratios, the Novomonastyrskoe deposit resembles the Kavalerovo deposits of similar type, which are constrained to the Taukha terrane (Fig. 6).

Being sufficiently representative, the data on the two large deposits of tin, lead and zinc (Yuzhnoye and Arsenievskoye) are of particular interest allowing assessment of the Pb isotope homogeneity.

The Yuzhnoe cassiterite-sulfide deposit (Krasnorechensk district) and Arsenyevskoe cassiterite-silicate-sulfide deposit (Kavalerovo district) occur in the Zhuravlevka turbidite complex. The mineralization at the Yuzhnoe deposit was dated to Late Cretaceous (95–90 Ma). The Arsenievskoe deposit was presumably formed in two stages (Finashin, 1986; Tomson et al., 1996; Gonevchuk et al., 2011): during the early (93–80 Ma) stage, the cassiterite-sulfide ore was formed, whereas during the late (60–55 Ma), the cassiterite-silicate-sulfide mineralization was emplaced. Thus, it is assumed that there is a significant (ca. 30 myr) time gap separating these two ore-forming stages. At the Arsenievskoe deposit, galena was analyzed from both early and late mineral assemblages (Table 2).

Notably when the TIMS technique was applied, the deposits, in which a variation level ($\nu$,%) of the Pb isotope ratio did not exceed 0.2%, were considered isotopically homogenous (Gulson, 1986). In galena from the both deposits, variation of Pb isotope ratios is less than the analytical error of the applied MC-ICP-MS technique: $\nu_{6/4}$, $\nu_{7/4}$ and $\nu_{8/4} < 0.02\%$. The presented results demonstrate significantly higher degree of homogeneity of the Pb isotope composition within individual deposits, due to specifics of the sources and genesis of the SSAP deposits. This homogeneity signature is revealed by application of the high accuracy isotope analysis. The variation magnitude of Pb isotope composition in the SSAP districts and in the entire subprovince is caused solely by differences (yet relatively small) of the Pb-isotope characteristics of the sources that formed the individual deposits. Within the Pb deposits themselves, the isotope composition is very homogenous ($\nu \leq 0.02\%$), and by a combination of $^{206}Pb/^{204}Pb$,

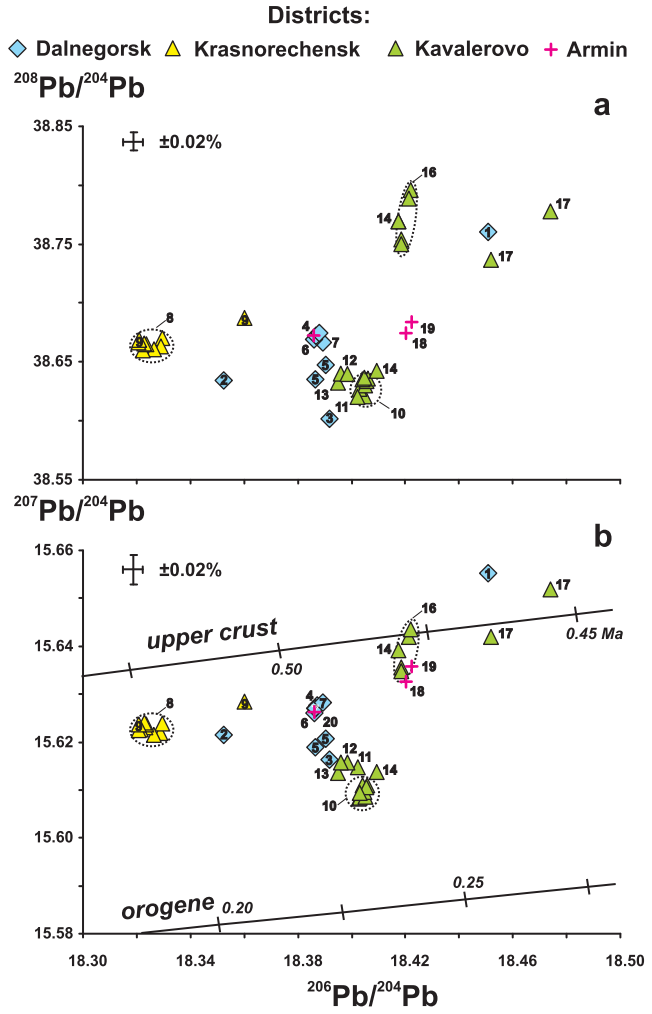


**Fig. 6.** Pb-Pb isotopic diagrams comparing lead isotope compositions of the SSAP deposits. Orogene and upper crust evolution curves (solid lines) are from Zartman and Doe (1981). The numbers on the diagrams correspond to the numbers of the SSAP deposits in Table 1.

$^{207}Pb/^{204}Pb$ and $^{208}Pb/^{204}Pb$ values it is individual. This distribution of Pb isotope composition data indicate that when ore deposition began, a matter in fluid-igneous sources of specific deposits reached a high degree of homogeneity with respect to the contents of U, Th and Pb and the isotopic composition of Pb and retained it until the mineralization process was completed.

The phenomenon of homogeneity of the Pb isotopic composition can be used for some geochronological estimates. For instance, formation of the two aforementioned mineral associations in the Arsenievskoe deposit was presumably separated by a 30 myr gap. The fact of high degree of Pb isotopic homogeneity in the galena of the early and late mineral associations clearly indicates Pb intake from the same source. During 30 myr (to the time of the late association formation), the values of all three Pb isotope ratios could grow due to accumulation of radiogenic $^{206}Pb$, $^{207}Pb$, and $^{208}Pb$ isotopes in the source's U-Th-Pb system. This can be assessed by calculation of a shift of $^{206}Pb/^{204}Pb$ ratio, since an effect of radiogenic $^{206}Pb$ growth is substantially larger (in 1.7 and 19 times) than that for the $^{207}Pb$ or $^{208}Pb$. To calculate the parameter μ ($^{238}U/^{204}Pb$), included in the well-known formula for calculating Δ ($^{206}Pb/^{204}Pb$), we took the value of U/Pb = 0.22 for the lead source. It represents an average U/Pb value in the Kavalerovo intrusive rocks (monzonites, granodiorites) (Gonevchuk, 2002) and does not differ much from average U/Pb values for the sedimentary rocks of Zhuravlevka terrane containing the Arsenievskoe deposit: U/Pb = 0.16 (Gonevchuk, 2002) and U/Pb = 0.17 (present work, Table 3). The value U/Pb = 0.22 corresponds to the value of the parameter $\mu = {}^{238}U/^{204}Pb = 13.8$.

It is evident from calculation that over the 30 myr period, $^{206}Pb/^{204}Pb$ in galena of the late mineral association would shift by 0.064 (or 0.35 rel.%). This result contradicts the fact of a high degree homogeneity and identity of Pb isotopic composition (including the $^{206}Pb/^{204}Pb$ ratio) in galena of the two mineralization stages, separated (supposedly) by 30 myr gap. The situation will not change fundamentally if the calculation of Δ ($^{206}Pb/^{204}Pb$) takes a lower value of μ, for example, μ = 10.8, corresponding to U/Pb = 0.17 in the Zhuravlevka terrane siliciclastics, or μ = 9.74 (average for the continental crust of the evolutionary model Stacey and Kramers (1975). Then Δ ($^{206}Pb/^{204}Pb$) would be 0.050 (or 0.27 rel.%) or 0.045 (or 0.24 rel.%), respectively. In any case, these virtual shifts are quite significant comparing to the lead isotope homogeneity at the Arsenievskoe deposit. The difference in average values of $^{206}Pb/^{204}Pb$ in the galena of these two uneven-aged mineral associations (early − 18.4049 ± 0.0010, late − 18.4039 ± 0.0010) is 0.001 (or 0.005 rel.%), which is 4 times less than the error of the applied MC-ICP-MS method. However, the error itself should be taken as a threshold of difference or similarity of the measured isotopic ratios, i.e., 0.02%, which in units of the $^{206}Pb/^{204}Pb$ ratio corresponds to 0.0037.

There is, possibly, the only explanation that eliminates the contradiction between the calculated and actual isotope shifts in the ore lead of the Arsenievskoe deposit: the time interval separating formation of the cassiterite-sulfide and cassiterite-silicate-sulfide mineral associations was actually much shorter than that estimated by K-Ar data and geological similarities. With the above discriminatory threshold of 0.0037 (or 0.02% rel.) for $^{206}Pb/^{204}Pb$ ratio, grounding upon the Δ ($^{206}Pb/^{204}Pb$) shifts calculated for different μ values, it can be shown that the time interval separating formation of the two mineral associations certainly could not exceed 2.5 myr.

### 6.2. General geochemical characteristics of the source of lead

The lead source of the SSAP deposits has average values of the evolutionary parameters ($\mu_2 = {}^{238}U/^{204}Pb = 9.78 \pm 0.05$ (SD), $\omega_2 = {}^{232}Th/^{204}Pb = 39.2 \pm 0.5$ (SD), $^{232}Th/^{238}U = 4.01 \pm 0.03$ (SD)), calculated by Stacey-Kramers's two-stage model (Stacey and Kramers, 1975): this corresponds to U-Th-Pb isotope systematics of the global geochemical crustal reservoir. One of the features of this source features is proximity of the $\mu_2$ parameter to the mean crustal value of 9.74 at elevated values of $^{232}Th/^{204}Pb$ and Th/U ratios. Taken together, these geochemical characteristics of the SSAP lead indicate that is was lead sourced most likely from the continental crust that passed the recycling stage, accompanied by a change in the evolutionary parameters of its U-Th-Pb systematics: both Th/Pb and Th/U grew up while U/Pb ratios have reduced. This assumption is consistent with the fact that Pb-Pb model age values are systematically older by ca. 100–200 myr compared with the actual geological age of the SSAP mineralization (Table 2, Fig. 7).

### 6.3. Assessing role of crustal and mantle sources in the genesis of the SSAP deposits

A Pb isotopic composition and its homogeneity degree in certain deposits or entire ore provinces was previously studied (Zartman, 1974; Macfarlane et al., 1990, Chernyshev and Shpikerman, 2001; Kamenov et al., 2002; Chugaev et al., 2013a; Chugaev and Chernyshev, 2017; Chernyshev et al., 2018) to depend on lead isotope characteristics in potential sources of lead from igneous and sedimentary rocks of tectonic blocks which host the deposits.

According to the existing concept, the SSAP deposits formationaly associate with the Late Cretaceous and Paleocene granitoid suites (Finashin, 1986; Tomson et al., 1996; Gonevchuk, 2002; Grebennikov

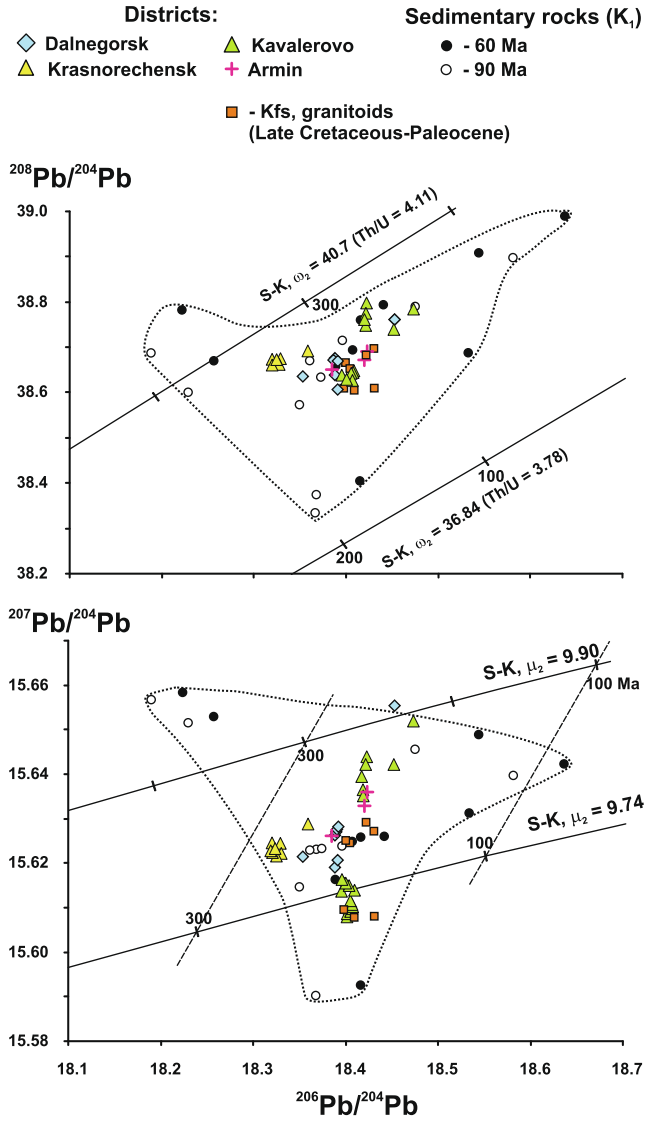


**Fig. 7.** Pb-Pb isotopic diagrams comparing lead isotopic composition of the SSAP deposits, Early Cretaceous sedimentary rocks of Zhuravlevka and Taukha complexes (Armin, Kavalerovo and Dalnegorsk districts), and K-feldspars from Late Cretaceous-Paleocene granitoids (Kavalerovo and Dalnegorsk districts). Solid lines correspond to evolutionary curves of Pb isotopic composition according to model of (Stacey and Kramers, 1975).

et al., 2016; Gonevchuk et al., 2011, etc.). It is assumed that the ore-forming processes, apart of a magmatic source, were also contributed by a fluid from host sedimentary complexes (Ratkin et al., 2016b).

The SSAP Pb isotopic composition was compared with an initial Pb isotopic composition of the Early Cretaceous sedimentary rocks from the Zhuravlevka and Taukha complexes, as well as feldspar fractions from the Late Cretaceous and Paleocene granitoids (Fig. 7). The feldspar points represent age-corrected Pb isotope ratios (see the Results section above). Each sedimentary rock sample is represented by two points, corresponding to 90 and 60 Ma corrected values. Both Pb-Pb diagrams show the evolution curves of the Pb isotope composition according to the Stacey-Kramers model.

In terms of Pb isotope ratios, the studied Late Cretaceous and Paleocene granitoids are similar to the Kavalerovo and Arminsky ore districts deposits: Pb isotope compositions of the granitoids and the SSAP deposits are largely combined and overlap in both Pb-Pb diagrams (Fig. 7a,b). The observed relations of the deposits and granitoids support those in the models of the SSAP deposits genesis that consider felsic melts as the main source of ore components (Korsunov, 1995; Gonevchuk, 2002, etc.).

At that, the shift of lead isotope composition of the deposits in the Pb-Pb diagrams relative to the igneous rocks suggests contribution from another source. This (with lead-isotope characteristics $\mu_2 \geq 9.9$, $\omega_2 \geq 39.9$) could be sourced from rocks of sedimentary complexes of the Taukha and Zhuravlevka terranes. Contribution of host rocks in the ore-forming process is repeatedly noted by researchers when studying Pb-Pb isotope systematics of hydrothermal deposits of different genesis and ore specialization (Beaudoin and Sangster, 1992; Paiement et al., 2012; Standish et al., 2014; Chugaev and Chernyshev, 2017, etc.). An important geochemical feature of the Taukha and Zhuravlevka sedimentary units, allowing to consider them as one of the possible sources, is an elevated concentration content of some ore components. For instance, the Early Cretaceous siliciclastics from the Zhuravlevka terrane flysch are typically enriched in lead (> 45 ppm), zinc (> 125 ppm), and boron (37–196 ppm). The tin content in them varies from 4 to 5 ppm (Kostin et al, 2006). Geochemical specialization, with Pb (31–158 ppm), Zn (52–194 ppm) and B (up to 150 ppm), is also observed for the Early Cretaceous arkose sandstones and Triassic chert from the Taukha terrane (Kostin et al, 2006). Feldspar, detrital tourmaline and biotite are considered as the main host minerals for Pb, B and Sn, respectively (Rostovsky and Khetchikov, 2000; Malinovsky and Golozubov, 2011).

The analyzed sedimentary rocks of the Zhuravlevka and Taukha complexes reveal significant heterogeneity in Pb isotope composition: their points are widely scattered on the Pb – Pb diagrams (Fig. 7). The points of the siliciclastics of the Zhuravlevka and Taukha complexes differ somewhat in their position on the diagrams. In the $^{206}Pb/^{204}Pb$ vs. $^{207}Pb/^{204}Pb$ diagram, the Taukha complex sandstone points are located in the upper part of the diagram, corresponding to high values of $\mu_2 = 9.9$. The points of the Zhuravlevka complex gravitate to the middle and lower parts of the diagram, suggesting that the U-Pb system of these rocks evolved for a long time at lower $\mu_2 = 9.64$–$9.79$, close to the mean crustal $\mu_2$ value. Taking into account similarity of sedimentation ages of the studied rocks of Zhuravlevka and Taukha terranes, it can be assumed that the observed differences in the Pb isotopic composition indicate different compositions and sources of siliciclastic material of these sedimentary units. According to modern geotectonic models, the main source of debris for the Taukha terrane rocks was the eastern part of the North China Craton particularly the Korean Peninsula rocks (Golozoubov, 2006; Liu et al., 2017). The Early Cretaceous sediments of the Zhuravlevka complex had a greater number of provenance areas being reconstructed: besides the North China Craton and the Korean Peninsula, the clastic material was also eroded from the Bureya-Jiamusi-Khanka superterrane (Kudymov and Medvedeva, 2012; Liu et al., 2017). It should be noted that various Precambrian complexes of deeply metamorphosed rocks occur in the proposed provenance areas (Wilde et al., 2002; Zhai et al., 2007; Zhao and Zhai, 2013; Wilde, 2015; Yang et al., 2017). In the $^{206}Pb/^{204}Pb$ vs. $^{208}Pb/^{204}Pb$ diagram, the points of the sedimentary rocks are located well above the average crustal evolutionary curve. This fact indicates an input of lead from ancient metamorphic rocks in the late recycling processes, as evidenced by the high model values of the $^{232}Th/^{204}Pb$ and Th/U ratios in the Pb source of the Early Cretaceous sedimentary strata of the Zhuravlevka and Taukha complexes.

The field of lead isotope composition of the sedimentary rocks of the Zhuravlevka and Taukha complexes overlaps with the points of lead isotope composition of all the studied SSAP deposits and the Late Cretaceous-Paleocene granitoids. This fact can be taken as the evidence that the sedimentary strata were one of the sources of lead to the ore-forming fluids.

The above results allow to conclude that at least two sources of supplied metals to the SSAP deposits. One of the sources is identified as granitic melts, and the other is the Mesozoic sedimentary complexes. The hydrothermal system of the deposits received Pb from both sources:

the high degree of lead isotopic homogenization was achieved via a mixing process. The available Pb-Pb data for igneous and sedimentary rocks of the region does not allow to quantify contribution of these sources to the ore formation of each studied SSAP deposits. The only exception is the Arsenievskoe deposit, where the identity of Pb isotope composition of the ores and spatially associated granitoids has been revealed (Fig. 7). This fact definitely indicates the leading role of the magmatic source in the genesis of this deposit. In general, Pb-Pb data confirm the genetic relationship of the ore formation and magmatism, during Late Cretaceous to Paleocene time.

Given the leading role of the granitoid magmatism in the SSAP formation, it is important to consider sources of felsic melts. During Late Cretaceous to Paleocene times, the granitic magmatism developed predominantly in active continental margin setting, set by subduction and left-lateral movements (transform mode) of the Paleo-Pacific Plate along the Paleo-Asian continental margin (Maruyama et al., 1997; Golozoubov, 2006; Grebennikov et al., 2016; Khanchuk et al., 2016). By this time, thick (up to 38 km) crust had been formed at the continental margin (Rodnikov et al., 2008). It comprises units of accretionary complexes composed of Triassic to Jurassic pelagic sediments, volcanic and siliciclastic (mainly arkose sandstones) rocks, Late Cretaceous flysch units, and rocks of Early Cretaceous island arcs. According to the geochemical and Sr-Nd isotope studies, the parental melts of the post-accretionary granitoids were contributed by both crustal and mantle sources (Gonevchuk, 2002; Kruk et al., 2014; Jahn et al., 2015; Khanchuk et al., 2016).

Jahn et al. (2015), have summarized Sm-Nd isotopic data and demonstrated that fraction of the crustal matter in the granitoid melts could range from 33 to 64%. These estimates are based on the assumption that an original mantle melt was contaminated by an old (Precambrian) continental crust, for which $\varepsilon_{Nd}(t) = -13$ was taken to the calculations (Jahn et al., 2015). However, available geological, geophysical and geochemical data do not confirm presence of any old continental crust under the accretionary sedimentary complexes of the Sikhote-Alin orogenic belt. On the contrary, a number of researchers prove that the belt is based upon oceanic crust (Golozoubov, 2006; Khanchuk et al., 2013; Petrischevsky, 2013; Kruk et al., 2014; Khanchuk et al., 2016). The petrological model developed by these authors demonstrates that oceanic basalts and sedimentary sequences of accretionary complexes were involved in the Cretaceous processes of granitoid melt formation (Kruk et al., 2014; Khanchuk et al., 2016). The sedimentary rock Sm-Nd isotope characteristics in different blocks of the Sikhote-Alin orogenic belt are very heterogeneous. The values of $\varepsilon_{Nd}(t)$ vary over a wide range from +1.4 to −18.4 (Kruk et al., 2014; Khanchuk et al., 2016, our data in Table 4). In the Late Cretaceous to Paleocene granitoids of SAOB, values of $\varepsilon_{Nd}(t)$ range from +2.1 to −4.2 (Jahn et al., 2015; Kruk et al., 2019). These significant variations

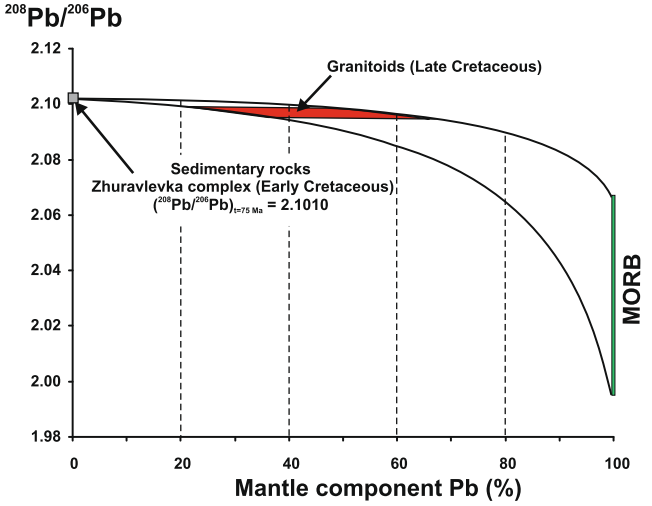


**Fig. 8.** Proportions of the mantle component Pb vs. $^{208}Pb/^{206}Pb$ plot for the Late Cretaceous granitoids from Kavalerovo ore district, Sikhote-Alin. Isotopic composition of Pb in MORB after (White et al., 1987; Cousens et al., 2017).

of $\varepsilon_{Nd}(t)$ make dubious any estimates of contribution of the sedimentary rocks to the granitic melts if based only on Sm-Nd isotopic data. The corresponding estimates, based on the Pb isotope composition of the sedimentary rocks of accretionary complexes and granitoids could be quite useful.

The model we used for this purpose was as follows. The granite forming process includes mixing of lead from two geochemical sources: crust and mantle. The crustal matter was involved in the felsic melts by anatectic melting of sedimentary rocks (Kruk et al., 2014; Khanchuk et al., 2016). In the case of Kavalerovo district, the crustal source of lead in granites is correlated with the Early Cretaceous sedimentary rocks of the Zhuravlevka complex, for which the most representative Pb-Pb data have been obtained. The second (mantle) source Pb-Pb characteristics were taken by analogy with those for the Pacific MORB. Contribution from this source is allowed in the genesis of Cretaceous granitoids. According to petrogenetic models, the Late Cretaceous granite formation involved metamorphosed oceanic basalts occurring at the base of the accretionary complexes, as well as basaltic blocks within the sedimentary strata (Kruk et al., 2019; Khanchuk et al., 2016). These limitations of the mixing model do not contradict the existing concepts about the Late Cretaceous granitoid genesis in the SSAP.

A shift of Pb isotopic composition in the granitic melts could be caused by oceanic sediments in a subduction zone. However, available geochemical and Pb-isotope data for the Early Cretaceous oceanic

**Table 4**
Sm–Nd isotopic data for Early Cretaceous sedimentary rocks of Zhuravlevka and Taukha terranes, Sikhote-Alin (Russian Far East).

| № | Sample | Sample description | Sm (ppm) | Nd (ppm) | $^{147}Sm/^{144}Nd$ (± 2SE) | $^{143}Nd/^{144}Nd$ (± 2SE) | $\varepsilon_{Nd(t)}$ | $T_{(DM)}$ Ga |
|---|---|---|---|---|---|---|---|---|
| *Taukha terrane* | | | | | | | | |
| Dalnegorsk district | | | | | | | | |
| 1 | 309/1 | Berriasian -Valanginian sandstone | 4.2 | 23.3 | 0.1082 ± 1 | 0.511863 ± 6 | −13.7 | 1.9 |
| 2 | 309/2 | Berriasian -Valanginian sandstone | 4.2 | 26.2 | 0.0974 ± 3 | 0.511753 ± 6 | −15.5 | 1.8 |
| *Zhuravlevka terrane* | | | | | | | | |
| Kavalerovo district | | | | | | | | |
| 3 | Zh-71 | Early-Middle Albian sandstone | 6.5 | 33.8 | 0.1166 ± 1 | 0.512054 ± 6 | −10.1 | 1.7 |
| 4 | Zh-82 | Middle-Late Albian sandstone | 6.3 | 32.0 | 0.1470 ± 1 | 0.512007 ± 6 | −11.7 | |
| 5 | Zhr −1 | Late Berriasian-Early Valanginian siltstone | 6.4 | 26.0 | 0.1099 ± 1 | 0.512274 ± 5 | −6.0 | 1.3 |
| 6 | Zhr −10 | Late Berriasian-Early Valanginian sandstone | 6.6 | 36.0 | 0.1075 ± 1 | 0.511852 ± 6 | −14.2 | 1.9 |
| 7 | Zhr-56/1 | Early-Middle Albian sandstone | 3.2 | 18.0 | 0.1039 ± 1 | 0.511785 ± 7 | −15.5 | 1.9 |

The values of $\varepsilon_{Nd(t)}$ were calculated using the following parameters of the uniform chondrite reservoir (CHUR): $^{147}Sm/^{144}Nd = 0.1967$, $^{143}Nd/^{144}Nd = 0.512638$ (Jacobsen and Wasserburg, 1984). The model age $T_{(DM)}$ was calculated using following parameters of the present-day depleted mantle (DM) = $^{147}Sm/^{144}Nd = 0.2137$, $^{143}Nd/^{144}Nd = 0.513151$ (Goldstein and Jacobsen, 1988).

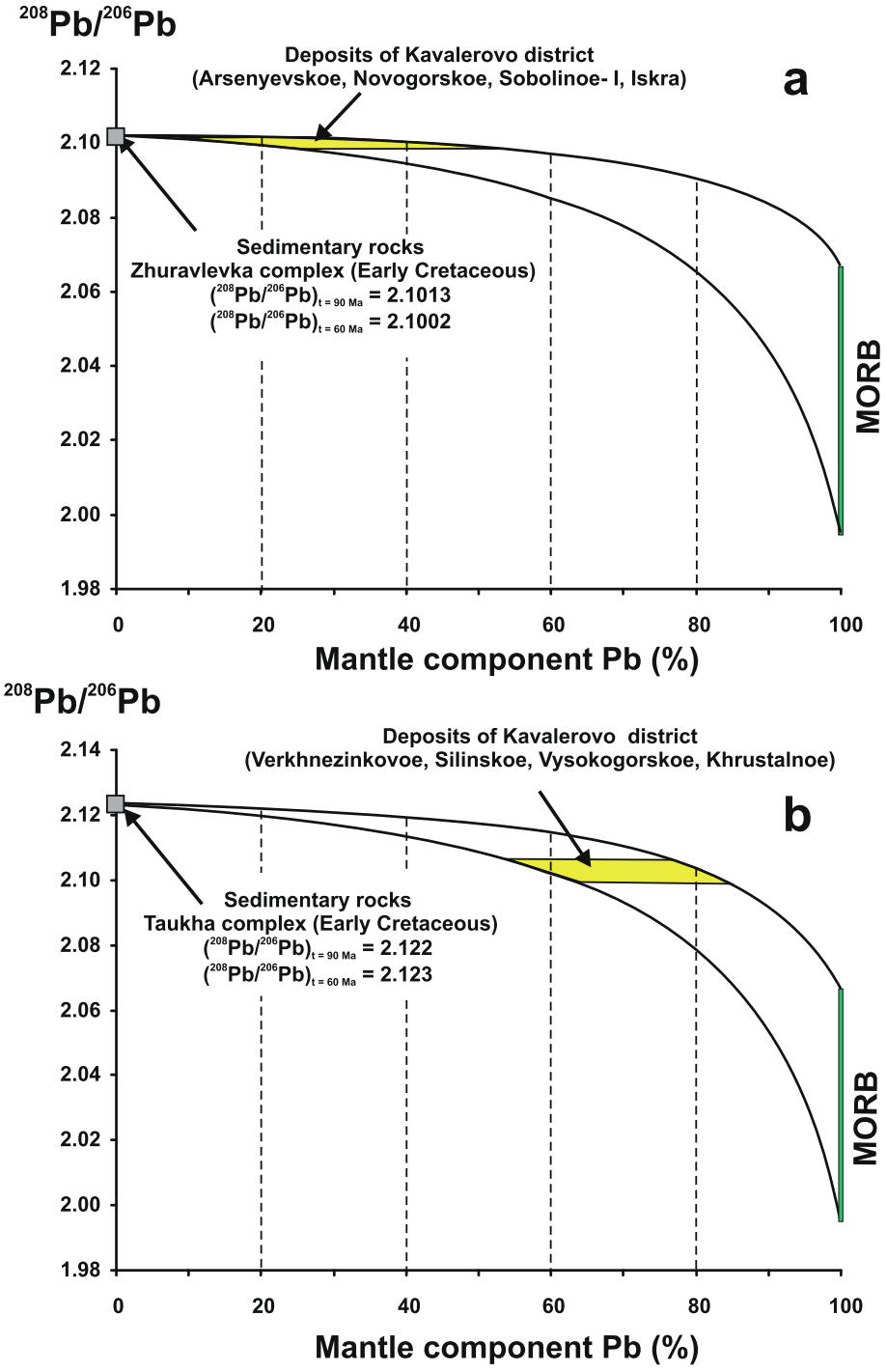


**Fig. 9.** Proportions of the mantle component Pb vs. $^{208}Pb/^{206}Pb$ plots for the deposits of Kavalerovo district, Sikhote-Alin. Isotopic composition of Pb in MORB after (White et al., 1987; Cousens et al., 2017).

sediments of the northwestern Pacific Ocean show that their average Pb content is several times less than in the sedimentary rocks of the Zhuravlevka complex, while their Pb isotopic compositions are similar (Kuroda et al., 2011). This allows us to neglect the oceanic sediments lead contribution in the model calculations.

The model was applied to the studied granitoids of the Kavalerovo district. The comparison parameter was the $^{208}Pb/^{206}Pb$ ratio, which best demonstrates discrepancy of the sedimentary rocks and MORB of the Pacific Ocean. For the crustal component, the lead content and $^{208}Pb/^{206}Pb$ ratio were taken to be equal to average values of the corresponding parameters in the sedimentary rocks of the Zhuravlevka complex of the Kavalerovo district: Pb = 15.58 ppm and $(^{208}Pb/^{206}Pb)_{av}$ = 2.101 ± 5 (SD). The average lead content in the North Pacific MORB was earlier estimated by Cousens et al. (2017). It should be noted that MORB of the Pacific Ocean demonstrates considerable heterogeneity of Pb isotope composition, including $^{208}Pb/^{206}Pb$ (White et al., 1987; Cousens et al., 2017). This fact was taken into account in model calculations where both the minimum and maximum values of this ratio were used ($^{208}Pb/^{206}Pb_{min}$ = 1.9952, $^{208}Pb/^{206}Pb_{max}$ = 2.0660).

According to the calculations, the Pb fraction of the crustal component in the granitoid melts of the studied Late Cretaceous intrusions

of the Kavalerovo district varies from 20 to 66% (Fig. 8), which generally agrees with the values obtained for the Late Cretaceous-Paleocene granitoids of the Sikhote-Alin orogenic belt considering their Sm-Nd systematics (Jahn et al., 2015).

This model was also applied to estimate proportions of the mantle and crustal Pb sources in the ores of the Kavalerovo district (Fig. 9). For the cassiterite-sulfide Late Cretaceous deposits of Arsenievskoe, Novogorskoe and Sobolinoe-I, hosted by the Zhuravlevka complex sediments, average mantle Pb contribution is estimated to be ca. 20–40% (Fig. 9a). In the cassiterite-silicate-sulfide Paleocene Iskra deposit, the mantle contribution is < 10%. The largest contribution (60–80%) of mantle lead has been found in the cassiterite-sulfide and cassiterite-silicate-sulfide ores from the Khrustalnoe, Vysokogorskoe, Verkhnezinkovoe and Silinskoe deposits located among the rocks of the Taukha complex in the eastern part of the Kavalerovo district (Fig. 9b). It is possible that a higher proportion of mantle lead in the eastern group of deposits in the Kavalerovo district might be caused by occurrence of oceanic basalts in the Taukha complex.

The above data are rough estimates, but they definitely indicate the contribution of lead from the sedimentary units in the ore formation process: these units were involved both in the granite and ore formation stage as a result of fluid-rock interaction. Along with this, an important role was played by a mantle-type source of lead, which contribution could be very significant in formation of many SSAP deposits.

## 7. Summary

The South Sikhote-Alin subprovince, spatially covering the Zhuravlevka and Taukha terranes of the SAOB, is one of the largest in the Russian Far East. It encompasses numerous deposits of tin, tungsten, lead, zinc, silver and boron, formed in the Late Cretaceous to the Paleocene during subduction and left-lateral movement of the Paleo-Pacific Plate along the Paleo-Asian continental margin.

The Pb-Pb study of 20 deposits, differing in age, tectonic setting and metallogenic specialization, showed that, in general, they have similar values of Pb isotopic ratios. The measured values of $^{206}Pb/^{204}Pb$, $^{207}Pb/^{204}Pb$ and $^{208}Pb/^{204}Pb$ vary in relatively narrow limits: from 18.321 to 18.474, from 15.608 to 15.655 and from 38.601 to 38.796, respectively. Notably, within the individual deposits, the Pb isotope composition is homogeneous, and the revealed variations do not exceed the analytical error ( ± 0.02%) of the employed MC-ICP-MS technique. Compared with the well-known metallogenic provinces of the Central Andes, Eastern Transbaikalia and Western Iran, the South Sikhote-Alin subprovince has significantly smaller variation scale ($\nu_{6/4}$ = 0.2%, $\nu_{7/4}$ = 0.08% and $\nu_{8/4}$ = 0.13%) of the Pb isotopes. The high degree of homogeneity of the Pb isotope composition and absence of correlations between the lead isotope characteristics of the deposits, on the one hand, and the age and type of ore mineralization, on the other, indicate the presence of a regional uniform Pb source for all the SSAP deposits. The results of Pb-Pb studies of rocks suggest that the source was most likely the Mesozoic sedimentary sequences of the Sikhote-Alin accretionary complexes.

The sedimentary rocks contributed both at the stage of generation of ore-bearing melts as a result of anatectic melting and/or dragging of sediments in the subduction zone, and at the stage of deposition of the mineralization by hydrothermal fluids. As a result of these processes, high degree of homogeneity of the Pb isotope composition was achieved in individual deposits and the entire metallogenic province. The geochemical specialization of sedimentary rocks in accretionary complexes on zinc, tin and boron suggests that they could be the source of other ore-forming components. In turn, the individual lead isotope characteristics of the SSAP deposits are caused not only by the Pb isotope compositional peculiarity of the sedimentary rocks in tectonic blocks.

A definite contribution to the overall balance of ore lead was also done by the mantle source lead, probably extracted from oceanic basalts forming the basement of the accretionary complexes, as well as those occurring as blocks among the sedimentary units. The contribution from the oceanic basalts is allowed by petrogenetic models developed for Late Cretaceous granitoids in the SAOB (Kruk et al., 2019; Khanchuk et al., 2016). Exemplified by the Kavalerovo deposits, it is shown that the contribution of lead from mantle source in some deposits could be reaching 60–80%.

## Declaration of Competing Interest

The authors declare that they have no known competing financial interests or personal relationships that could have appeared to influence the work reported in this paper.

## Acknowledgments

We are grateful to the reviewer for the constructive comments that have improved the article. This research was financially supported by the Program of the Russian Academy of Sciences N 48, State Contract No 0136-2016-0037 and by the Ministry of Science and Higher Education of the Russian Federation contract No. 14.Y26.31.0029 in the framework of the Resolution No.220 of the Government of the Russian Federation.

## Appendix A. Supplementary data

Supplementary data to this article can be found online at https://doi.org/10.1016/j.oregeorev.2020.103683.

## References

Alenicheva, A.A., Sakhno, V.G., 2008. The U-Pb dating of extrusive-intrusive complexes in ore districts in the southern part of the Eastern Sikhote-Alin Volcanic Belt (Russia). Dokl. Earth Sci. 419, 217–221. https://doi.org/10.1134/S1028334X08020062.

Bazhanov, V.A., Oleynik, Yu.A., 1989. Geological map of Prymorsky kray on a scale of 1:1000000. Magadan: SEPGA. 2 sheets.

Beaudoin, G., Sangster, D.F., 1992. A descriptive model for silver-lead-zinc veins in clastic metasedimentary terranes. Econ. Geol. 87, 1005–1021. https://doi.org/10.2113/gsecongeo.87.4.1005.

Belyatsky, B.V., Vinogradova, L.G., Krymsky, R.S., Levsky, L.K., 1994. Sm-Nd and Rb-Sr isotope dating of wolframite-rare-metal deposit Zabytoe. Prymorye. Petrol. 2, 243–250 (in Russian).

Chernyshev, I.V., Chugaev, A.V., Bortnikov, N.S., Gamyanin, G.N., Prokopiev, A.V., 2018. Isotopic composition of lead and metal sources in the gold and silver deposits of South Verkhoyanye (Yakutia, Russia): according to the data of the highly precise MC-ICP-MS method. Geol. Ore Deposits 60, 398–417. https://doi.org/10.1134/S1075701518050033.

Chernyshev, I.V., Chugaev, A.V., Shatagin, K.N., 2007. High-precision Pb isotope analysis by multicollector-ICP-mass-spectrometry using $^{205}Tl/^{203}Tl$ normalization: optimization and calibration of the method for the studies of Pb isotope variations. Geochem. Int. 45, 1065–1076. https://doi.org/10.1134/S0016702907110018.

Chernyshev, I.V., Shpikerman, V.I., 2001. The isotopic composition of ore-hosted lead as a reflection of the block structure of Central Northeastern Asia. Dokl. Earth Sci. 377, 337–340.

Chugaev, A.V., Chernyshev, I.V., 2017. Pb–Pb isotopic systematics of orogenic gold deposits of the Baikal-Patom fold belt (Northern Transbaikalia, Russia) and estimation of the role of neoproterozoic crust in their formation. Geochem. Int. 55, 1010–1021. https://doi.org/10.1134/S0016702917110040.

Chugaev, A.V., Chernyshev, I.V., Bortnikov, N.S., Kovalenker, V.A., Kiseleva, G.D., Prokof'ev, V.Y., 2013a. Lead isotope ore provinces of eastern Transbaikalia and their relationships to regional structures: results of high-precision MC-ICP-MS study of Pb isotopes. Geol. Ore Deposits 55, 245–255. https://doi.org/10.1134/S107570151304003X.

Chugaev, A.V., Chernyshev, I.V., Lebedev, V.A., Eremina, A.V., 2013b. Lead Isotope composition and origin of the quaternary lavas of Elbrus Volcano, the Greater Caucasus: high-precision MC-ICP-MS data. Petrology 21, 16–27. https://doi.org/10.1134/S0869591113010037.

Collerson, K.D., Kamber, B.S., Schoenberg, R., 2002. Applications of accurate, high precision Pb isotope ratio measurement by multi-collector ICP-MS. Chem. Geol. 188, 65–83. https://doi.org/10.1016/S0009-2541(02)00059-1.

Cousens, B., Weis, D., Constantin, M., Scott, S., 2017. Radiogenic isotopes in enriched mid-ocean ridge basalts from Explorer Ridge, northeast Pacific Ocean. Geochim. Cosmochim. Acta 213, 63–90. https://doi.org/10.1016/j.gca.2017.06.032.

Didenko, A.N., Arkhipov, M.V., Oto, Sh., Golozoubov, V.V., Kudymov, A.V., Voynova, I. P., Peskov, A.Yu., 2018. Geochronology, paleomagnetism of Silasinskaya and Kemskaya formations of Sikhote-Alin: comparative analysis, in: Geological

Processesin the Lithospheric Plates Subduction, Collision, and Plate Environments. Proceedings of IV Russian scientific conference with foreign participants. Vladivostok. Russia. 29–32. (in Russian).
Finashin, V.K., 1986. Tin ore deposits of Primorye. Vladivostok: FEBASUSSR. (in Russian).
Goldstein, S.J., Jacobsen, S.B., 1988. Nd and Sr isotopic systematic of river water suspended material: implications for crustal evolution. Earth Planet. Sci. Lett. 87 (3), 249–265. https://doi.org/10.1016/0012-821X(88)90013-1.
Golozoubov, V.V., 2006. Tectonics of the Jurassic and Lower Cretaceous complexes of the north-western framing of the Pacific ocean. Dalnauka, Vladivostok (in Russian).
Gonevchuk, V.G., 2002. Tin-bearing systems of the Far East: magmatism and ore genesis, Vladivostok: Dalnauka. (in Russian).
Gonevchuk, V.G., Korostelev, P.G., Semenyak, B.I., Gonevchuk,G.A., Gorelikova N.V., 2011. Tin-bearing systems of active margins; characteristics of genesis and ore presence, in: Geological Processes in the Lithospheric Plates Subduction, Collision, and Plate Environments. Proceedings of the Russian scientific conference with foreign participants. Vladivostok. Russia. 342–344. (in Russian).
Gonevchuk, V.G., Gonevchuk, G.A., Kokorin, A.M., Orekhov, A.A., Lebedev, V.A., 2005. New isotope-geochronological data, and some genesis problems of tin mineralization of Kavalerovo district (Primorye, Russia). Russian J. Pacific Geol. 24, 77–87 (in Russian).
Grebennikov, A.V., Khanchuk, A.I., Gonevchuk, V.G., Kovalenko, S.V., 2016. Cretaceous and Paleogenegranitoid suites of the Sikhote-Alin area (Far East Russia): geochemistry and tectonic implications. Lithos 261, 250–261. https://doi.org/10.1016/j.lithos.2015.12.020.
Gulson, B.L., 1986. Lead isotopes in mineral exploration. Amsterdam: Elsevier. Developments in Economic Geology Series no. 23. XII. 245 pp. DOI: 10.1017/S001675680000964X.
Jacobsen, S.B., Wasserburg, G.J., 1984. Sm-Nd isotopic evolution of chondrites and achondrites. Earth Planet. Sci. Lett. 67, 137–150. https://doi.org/10.1016/0012-821X(84)90109-2.
Jahn, B.M., Valui, G., Kruk, N., Gonevchuk, V., Usuki, M., Wu, J.T.J., 2015. Emplacement ages, geochemical and Sr–Nd–Hf isotopic characterization of Mesozoic to early Cenozoic granitoids of the Sikhote-Alin Orogenic Belt, Russian Far East: crustal growth and regional tectonic evolution. J. Asian Earth Sci. 111, 872–918. https://doi.org/10.1016/j.jseaes.2015.08.012.
Kamenov, G.D., Macfarlane, A.W., Riciputi, L., 2002. Sources of lead in the San Cristobal, Pulacayo, and Potosi mining districts, Bolivia, and a reevaluation of regional ore lead isotope provinces. Econ. Geol. 97, 573–592. https://doi.org/10.2113/97.3.573.
Kazachenko, V.T., Khanchuk, A.I., Lavrik, S.N., Perevoznikova, E.V., 2013. Phlogopite-olivine rocks of the Taukha terrane in southeastern Sikhote Alin. Russian J. Pacific Geol. 7 (5), 330–345. https://doi.org/10.1134/S1819714013050047.
Kemkin, I.V., 2006. Geodynamic evolution of Sikhote-Alin and the Sea of Japan region during the Mesozoic. M. Science (in Russian).
Khanchuk, A.I., Kemkin, I.V., Kruk, N.N., 2016. The Sikhote-Alinorogenic belt, Russian South East: terranes and the formation of continental lithosphere based on geological and isotopic data. J. Asian Eart Sci. 120, 117–138. https://doi.org/10.1016/j.jseaes.2015.10.023.
Khanchuk, A.I., Kruk, N.N., Golozoubov, V.V., Kovach, V.P., Serov, P.A., Kholodnov, V.V., Gvozdev, V.I., Kasatkin, S.A., 2013. The nature of the continental crust of Sikhote-Alin as evidenced from the Nb isotopy of rocks of Southern Primorie. Dokl. Earth Sci. 451, 809–813. https://doi.org/10.1134/S1028334X13080011.
Kokorin, A.M., Gonevchuk, V.G., Kokorin, D.K., Orekhov, A.A., 2001. The Vysokogorskoe tin ore deposit: mineralization and genesis characteristics, in: Ore deposits of the continental margins. Ed. 2. Vladivostok: Dalnauka. 156–171 (in Russian).
Korsunov, E.N., 1995. Magmatogenic ore systems and lead-zinc mineralization of the Dalnegorsky district. Soviet Geol. 11, 23–30 (in Russian).
Kostin, A.Ya., Korolev, V.N., Pezhenina, L.A., Losiv, V.N., Golozubov, V.V., 2006.State geological map on a scale of 1:200000 Second edition. South Sikhote-Alin series. Page L-53-XXXIV, XXXV (Dalnegorsk). Explanatory note. Saint-Petersburg: VSEGEI (in Russian).
Kruk, N.N., Gvozdev, V.I., Orekhov, A.A., Kruk, E.A., Kasatkin, S.A., Golozubov, V.V., Rudnev, S.N., Aoki, S.h., Komiya, T.I., Kovach, V.P., Serov, P.A., 2019. Early Cretaceous Granitic and Monzonitic Rocks of the Southern Part of the Zhuravlevka Terrane (Sikhote-Alin): Geochemical Composition and Melt Sources. Russ. J. Pacific Geol. 13, 220–238. https://doi.org/10.1134/S1819714019030047.
Kruk, N.N., Simanenko, V.P., Gvozdev, V.I., Golozoubov, V.V., Kovach, V.P., Serov, P.I., Kholodnov, V.V., Moskalenko, E.Y., Kuibida, M.L., 2014. Early Cretaceous granitoids of the Samarka terrane (Sikhote-Alin): geochemistry and sources of melts. Russ. Geol. Geophys. 55, 216–236. https://doi.org/10.1016/j.rgg.2014.01.007.
Kudymov, A.V., Medvedeva, S.A., 2012. Provenance of the Middle Jurassic-Lower Cretaceous (Berriasian-Valanginian) deposits of the Lower Amur region. Russian J. Pacific Geol. 6, 230–241. https://doi.org/10.1134/S1819714012030025.
Kuroda, J., Tanimizu, M., Hori, R.S., Suzuki, K., Ogawa, N.O., Tejada, M.L.G., Coffin, M.F., Coccioni, R., Erba, E., Ohkouchi, N., 2011. Lead isotopic record of Barremian-Aptian marine sediments: implications for large igneous provinces and the Aptian climatic crisis. Earth Planet. Sci. Lett. 307, 126–134. https://doi.org/10.1016/j.epsl.2011.04.021.
Liu, K., Zhang, J., Wilde, S.A., Liu, S., Guo, F., Kasatkin, S.A., Golozoubov, V.V., Ge, M., Wang, M., Wang, J., 2017. U-Pb Dating and Lu-Hf isotopes of detrital zircons from the southern Sikhote-alinorogenic belt, Russian Far East: tectonic implications for the early cretaceous evolution of the Northwest Pacific Margin. Tectonics 36, 2555–2598. https://doi.org/10.1002/2017TC004599.
Macfarlane, A.W., Marcet, P., Le Huray, A.P., Petersen, U., 1990. Lead isotope provinces of central Andes inferred from ores and crustal rocks. Econ. Geol. 85, 1857–1880. https://doi.org/10.2113/gsecongeo.85.8.1857.
Malinovsky, A.I., Golozubov, V.V., 2011. Lithology and depositional settings of the terrigenous sediments along transform plate boundaries: Evidence from the early cretaceous Zhuravlevka terrane in Southern SikhoteAlin. Russian J. Pacific Geol. 30, 35–52. https://doi.org/10.1134/S1819714011050058.
Maruyama, S., Isozaki, Y., Kimura, G., Terabayashi, M., 1997. Paleogeographic maps of the Japanese Islands: plate tectonic synthesis from 750 Ma to the present. Isl. Arc 6, 121–142. https://doi.org/10.1111/j.1440-1738.1997.tb00043.x.
Mirnejad, H., Simonetti, A., Molasalehi, F., 2011. Pb isotopic compositions of some Zn–Pb deposits and occurrences from Urumieh-Dokhtar and Sanandaj-Sirjan zones in Iran. Ore Geol. Rev. 39, 181–187. https://doi.org/10.1016/j.oregeorev.2011.02.002.
Nekrasov, I.Ya., Popov, V.K., 1990. On the step-like mechanism of the ore substance concentration in the Arsenievsky tin ore deposit as an example. Proceeding of the AS of USSR. 15, 1437–1442. (in Russian).
Nokleberg, W. (Ed.), 2010. Metallogenesis and Tectonics of Northeast Asia. CD-ROM.
Paiement, J.-P., Beaudoin, G., Paradis, S., Ullrich, T., 2012. Geochemistry and Metallogeny of Ag-Pb-Zn Veins in the Purcell Basin, British Columbia. Econ. Geol. 107, 1303–1320. https://doi.org/10.2113/econgeo.107.6.1303.
Petrischevsky, A.M., 2013. Gravity method of assessing rheological properties of Earth's crust. M.: Nauka (in Russian).
Radkevich, E.A., Tomson, I.N., Kokorin, A.M., Narboot, G.B., Finashin, V.K., Korenbaum, S.A., Kokorina, D.K., Anakhov, V.V., Osipova, G.A., Polokhov, V.P., Polaykova, O.P., Seliverstova, V.A., Seredin, V.V., Hilik, B.A., 1980. Zonality and depth of tin mineralization (in the Kavalerovsky district as an example). M.: Nauka (in Russian).
Rasskazov, S.V., Ivanov, V.V., Khanchuk, A.I., Chaschin, A.A., Fefelov, N.N., Saranina, E.V., 2002. Isotopic heterogeneity of Primorye ore deposits' galena lead. Proc. Acad. Sci. 387, 685 (in Russian).
Ratkin, V.V., Eliseeva, O.A., Pandian, M.S., Orekhov, A.A., Mohapatra, M., Vishnu Priya, S.K., 2018. Stages and formation conditions of productive mineral associations of the Dalnegorsk Borosilicate Deposit, Sikhote Alin. Geol. Ore Deposits 60, 672–684. https://doi.org/10.1134/S107570151808007X.
Ratkin, V.V., Karas, O.A., Golozubov, V.V., 2016a. Genesis of the boron potential of the Taukha metallogenic zone, Sikhote Alin, and boron sources during formation of the Dal'negorsk boron deposit. Russian J. Pacific Geol. 10, 443–457. https://doi.org/10.1134/S1819714016060063.
Ratkin, V.V., Simanenko, L.F., Eliseeva, O.A., 2016b. Types of deposits and resource potential of lead-zinc and borosilicate ores of the Dalnegorsk ore district (Sikhote-Alin). Russian Geol. 4, 1–13 (in Russian).
Rehkämper, M., Halliday, A.M., 1998. Accuracy and long-term reproducibility of lead isotopic measurements by MC-ICP-MS using an external method for correction of mass discrimination. Int. J. Mass Spec. 181, 123–133. https://doi.org/10.1016/S1387-3806(98)14170-2.
Rodnikov, A.G., Sergeyeva, N.A., Zabarinskaya, L.P., Filatova, N.I., Piip, V.B., Rashidov, V.A., 2008. The deep structure of active continental margins of the Far East (Russia). Russ. J. Earth Sci. 10, ES4002. https://doi.org/10.2205/2007ES000224.
Rostovsky, F.I., 2005. Pb isotope ratio of the ore leads of Eastern Asia. Russian J. Pacific Geol. 24, 33–45 (in Russian).
Rostovsky, F.I., Khetchikov, L.N., 2000. Rifting and regeneration of ore components in the process of the Sikhote-Alin sulfide-cassiterite mineralization's formation, in: Ore deposits of the continental margins. Vladivostok: Dalnauka, Issue 1. 113–123. (in Russian).
Shafiei, B., 2010. Lead isotope signatures of the igneous rocks and porphyry copper deposits from the Kerman Cenozoic magmatic arc (SE Iran), and their magmatic-metallogenetic implications. Ore Geol. Rev. 38, 27–36. https://doi.org/10.1016/j.oregeorev.2010.05.004.
Stacey, J.S., Kramers, I.D., 1975. Approximation of terrestrial lead isotope evolution by a two-stage model. Earth Planet. Sci. Lett. 26, 207–221. https://doi.org/10.1016/0012-821X(75)90088-6.
Standish, C.D., Dhuime, B., Chapman, R.J., Hawkesworth, C.J., Pike, A.W.G., 2014. The genesis of gold mineralisation hosted by orogenic belts: a lead isotope investigation of Irish gold deposits. Chem. Geol. 378, 40–51. https://doi.org/10.1016/j.chemgeo.2014.04.012.
Tomson, I.N., Polokhov, V.P., Polyakova, O.P., Mityushkin, N.T., Nosik, L.P., Chernyshev, I.V., 1984. Analysis of the tin sources of the Kavalerovoore region (South Primorye). In: Substance sources and the conditions of locating tin ore deposits. M.: Science. 104-124. (in Russian).
Tomson, I.N., Tananaeva, G.A., Polokhov, V.P., 1996. Mutual relations of different types of tin mineralization in the southern Sikhote-Alin (Russia). Geol. Ore Deposits 38, 357–372 (in Russian).
Valuy, G.A., Strizhkova, A.A., 1997. Petrology of shallow-depth granitoids on the example of Dalnegorsk district. Dalnauka, Primorye, Vladivostok (in Russian).
White, W.M., Hofmann, A.W., Puchelt, H., 1987. Isotope geochemistry of Pacific mid-ocean ridge basalt. J. Geophys. Res. 92, 4881–4893. https://doi.org/10.1029/JB092iB06p04881.
Wilde, S.A., 2015. Final amalgamation of the Central Asian Orogenic Belt in NE China: Paleo-Asian Ocean closure versus Paleo-Pacific plate subduction — a review of the evidence. Tectonophysics 662, 345–362. https://doi.org/10.1016/j.tecto.2015.05.006.
Wilde, S.A., Zhao, G., Sun, M., 2002. Development of the North China Craton during the late Archaean and its final amalgamation at 1.8 Ga: some speculations on its position within a global Palaeoproterozoic supercontinent. Gondwana Res. 5, 85–94. https://doi.org/10.1016/S1342-937X(05)70892-3.
Yang, H., Ge, W., Zhao, G., Bi, J., Wang, Z., Dong, Y., Xu, W., 2017. Zircon U-Pb ages and geochemistry of newly discovered Neoproterozoicorthogneisses in the Mishan region, NE China: constraints on the high-grade metamorphism and tectonic affinity of the Jiamusi-Khanka Block. Lithos 268, 16–31. https://doi.org/10.1016/j.lithos.2016.10.017.

Zartman, R.E., 1974. Lead isotopic provinces in the Cordillera of the Western United States. Econ. Geol. 69, 792–805. https://doi.org/10.2113/gsecongeo.69.6.792.
Zartman, R.E., Doe, B.R., 1981. Plumbotectonics – the model. Tectonophysics 75, 135–162. https://doi.org/10.1016/0040-1951(81)90213-4.
Zhai, M.G., Guo, J.H., Peng, P., Hu, B., 2007. U-Pb zircon age dating of a rapakivi granite batholith in Rangnim massif, North Korea. Geol. Magaz. 114, 547–552. https://doi.org/10.1017/S0016756807003287.
Zhao, G., Zhai, M., 2013. Lithotectonic elements of Precambrian basement in the North China Craton: review and tectonic implications. Gondwana Res. 23, 1207–1240. https://doi.org/10.1016/j.gr.2012.08.016.